AN ABSTRACT OF THE THESIS OF

Arthur J. Fisher for the degree of Master of Science in Soil Science
presented on November 16, 2012
Title: Evaporation Synergy in a Bi-Textured Soil System

Abstract approved:

_____

Maria I. Dragila

Evaporation synergy is the phenomenon in which two porous medium textures that share a common vertical boundary experience a higher cumulative evaporation than either homogeneous texture can produce. Studies that have been conducted to date address this phenomenon in relatively fine and coarse sands but not in finer textured soils where viscous forces play a major role. The purpose of this study was to determine which of the 66 combinations of soil textures would exhibit evaporation synergy and develop a conceptual model of the conditions necessary for synergy. The numerical modeler HYDRUS was used to investigate all soil texture combinations and generate evaporation rates and cumulative evaporation amounts for each system. In addition, two combinations of soils were selected as laboratory experiments based on the HYDRUS predictions: one that exhibited synergy (Loamy Sand & Silt Loam) and one that did not (Loamy Sand & Sandy Clay). The laboratory data supported the HYDRUS predictions for evaporation synergy and non-synergy. The conditions necessary for evaporation synergy were developed from the numerical and physical models' predictions and results. The two textures must experience different air-entry values to create lateral

and vertical pressure gradients, the fine must possess a high enough hydraulic conductivity to allow water to move to its surface before it reaches its own air-entry value and possess the capillarity to maintain liquid film flow to its surface, and the viscous forces within the coarse must be low enough for water to be pulled from itself to the fine. It was also determined that the evaporation rate of a bi-texture decreases as a series of constant-rate steps until the fine enters S2 evaporation and is associated with a stepwise recession of the drying front in the coarse media. The duration of each step appears to be associated with the lateral distance from which water can be extracted within the coarse media.

Evaporation Synergy in a Bi-Textured Soil System

by

Arthur J. Fisher

A THESIS

submitted to

Oregon State University

in partial fulfillment of

the requirements for the

degree of

Master of Science

Presented November 16, 2012

Commencement June 2013

<u>Master of Science</u> thesis of <u>Arthur J. Fisher</u> presented on <u>November 16, 2012.</u>

APPROVED:

_____

Major Professor, representing Soil Science

_____

Head of the Department of Crop and Soil Science

_____

Dean of the Graduate School

I understand that my thesis will become part of the permanent collection of Oregon State University libraries. My signature below authorizes release of my thesis to any reader upon request.

_____

Arthur J. Fisher, Author

CONTRIBUTION OF AUTHORS

Dr. Maria Dragila assisted with HYDRUS data collection and interpretation of data.

TABLE OF CONTENTS

LIST OF FIGURES

LIST OF FIGURES (Continued)

LIST OF TABLES

LIST OF APPENDIX FIGURES

I dedicate this work to my beautiful wife, Megan, whose love and support enabled me to challenge myself and to my major professor, Maria Dragila, whose guidance and teaching enabled me to succeed.

1.   Introduction to Evaporation from Heterogeneous Porous Media

Soil evaporation on a small scale may seem trivial to those who are not aware of the importance of how miniscule components affect the hydrologic cycle at a landscape scale. Small-scale studies involving evaporation fronts and the pressure gradients involved (Shaw, 1987), the effect of hydrophobicity on the evaporation front (Shokri et al., 2009), film flow connecting the drying front into the porous media (Yiotis et al., 2004), and varying evaporativity rates resulting in different cumulative evaporation amounts from the same porous media (Phillip, 1957) all reveals the importance of understanding the mechanisms of soil-water evaporation so that it may be applied to larger and numerous interests. These previous studies involve evaporation from homogeneous porous media and it is only recently that similar studies have begun to concentrate on heterogeneous media. Lehmann and Or (2009), Or (et al., 2007), Pillai (et al., 2009), Sharaeeni and Or (2010 and 2011), and Shokri (et al., 2010) have all conducted studies with evaporation from heterogeneous porous media where two textures share a common vertical boundary and have found an early air-entry in the coarse while the fine remains saturated and the system remains in stage 1 evaporation for an extended period of time. This extension of stage 1 evaporation results in an increase in net cumulative evaporation from the heterogeneous system that is greater than either homogeneous texture can produce and will hence be referred to as "evaporation synergy." Real-world applications could range from reducing groundwater contamination to water harvesting in dry agricultural settings. Cliffs and soil cracks often cut across multiple horizons with distinct textural properties that could result in similar evaporation mechanisms. Enhanced evaporation rate could be used to reduce groundwater contamination in

dairy effluent applications by minimizing the amount of percolation. In semi-arid agriculture, water harvesting by lateral transfer of water combined with evaporation suppression could be implemented by well-selected finer texture in planting strips with coarser texture natural soil in adjacent strips

2.   Literature Review: Technical Background on Mechanisms Controlling Evaporation from Soil Media

The process of evaporation from a porous medium requires a vapor pressure difference between the soil water and the atmosphere (Lehmann et al., 2006). The evaporation rate is affected by both atmospheric demand (humidity, temperature, and velocity of ambient air) and later by porous-medium pore space and transport properties (thermal and hydraulic conductivities and vapor diffusion) (Lehmann et al., 2008). A saturated porous medium will initially evaporate at a maximum potential rate (e_0) that is not regulated by porous-medium properties but by atmospheric demand. During the initial stage, water is pulled upwards towards the evaporation surface by the increasing suction from the soil-air interface. As tension increases, air invades the system via the larger pores, (Yiotis et al., 2006) called this the "initial drying period". During this first phase, the media is still able to supply the atmospheric demand, even with a partially dry surface. Water continues to move to the evaporation surface drawn by a continually increasing capillary pressure gradient; the increase in the gradient is necessary to compensate for the decrease in hydraulic conductivity as the soil surface dries out. This stage will continue until the tension at the surface is greater than the air entry of the smallest pores, film rupture occurs at this stage, a matric potential value herewith called the 'critical' value. This marks the end of stage 1 evaporation and the beginning of

Stage 2, where evaporation is soil profile controlled, also known as the falling rate period Hillel, 1998).

(Metzger and Tsotsas, 2005) describes the isothermal drying process as a series of emptying capillary tubes in which the largest capillaries empty first and are supplied by smaller capillaries. As the larger capillaries drain they exert pressure on the smaller capillaries until the smallest capillary begins to recede. At this point there is no high pressure from another water-supplying capillary and the drying rate decreases marking the end of stage 1 drying (Figure 1 in Metzger and Tsotsas, 2005).

This description of a cascading sequence highlights the role of the pore size distribution within the porous media. Metzger and Tsotsas (Equation 5 2005) points out that drying behavior depends strongly on the standard deviation of the distribution, whereas the size of the pores has negligible influence. This explains the increase in the period of the constant drying rate (stage 1) for media with a wider pore size distribution. In general, porous media with broad pore size distributions or with a binary pore size distribution, i.e., having micro and macropores, will dry more deeply (with an extended first drying period) than porous media with a narrow pore size distribution.

The connection between capillaries and drying rates are also discussed by (Shokri et al., 2010) where a continuous capillary liquid pathway is maintained while a drying front recedes into the porous medium during stage 1 evaporation in which "evaporative chimneys" supply the bulk of the evaporative demand. Their results show that even in coarse sand liquid phase continuity was maintained during partial air entry and hydraulic conductivity was not limiting the evaporative flux, sustaining Stage 1. Furthermore, at later stages of drying when the upper portion of the medium is at a lower moisture content the evaporative chimneys still

provided a liquid phase connection through the entire sample. The evaporative chimneys exist due to the random processes of penetration, expansion, and erosion that cause the fractal geometry of the drying front. This is why the liquid front does not increase evenly with decreasing Ca but in random fluctuations (Vorhauer et al., 2010).

The finger flow process further explains the evaporative chimney idea. The opposing forces of gravity and matric potential along with structural features such as macropores and fractures create unstable flows and fingering within the porous medium. These forces can be quantified by the dimensionless Bond (Bo) and Capillary (Ca) numbers where Bond number expresses the relative importance of gravitational to capillary forces and the capillary number reflects the relative importance of viscous to capillary forces (Or, 2008). When water is displaced by air (drainage), viscosity increases the flow instability and when air is displaced by water (imbibition), viscosity has a stabilizing effect (Carminati (b) et al., 2007). Hence, different values for Bo and Ca will determine whether or not finger flow will result in the porous medium.

Similar to finger flow Yiotis et al. (2003) have shown that film flow accelerates drying significantly as Ca decreases. Film flow is different from conventional drying where a menisci spanning a pore-throat moves toward the evaporating surface due to a pressure gradient in the capillaries. Instead, film flow is the movement of micro and macroscopic liquid films along the pore surface and provides hydraulic conductivity that can be important in the transport of mass. Further experiments with film flow reinforce its major role in the drying of porous material even in nonisothermal conditions. Film flow has a dominant effect over temperature (unless film flow is very small) and when capillarity controls the process, which is what happens in most cases (Yiotis et al., 2004). Yiotis et al.,

(2007) have also found that as long as the liquid films span across the entire pore network they will provide hydraulic conductivity between the bulk liquid front and the drying surface extending stage 1 evaporation (Figure 2).

Many experiments involving media heterogeneities at a laboratory scale have been conducted to develop a better understanding of how water and solutes travel and drain from the vadose zone. Ursino et al., (2001) found that low saturation in a 2D cross section of randomly layered sand sized cubes led to a large transport heterogeneity and strong preferential flow. In fact, the macroscopic anisotropy that is a major element of transport in unsaturated media is very much saturation dependent and the direction of the mean trajectory varied with different water fluxes. In other words, the direction of flow deviated from the applied gradient with decreasing saturation. Ursino and Gimmi (2004) later confirmed the feasibility of characterizing and describing conductivity patterns in such soils with sharp conductivity (textural) contrasts. However, despite having the conductivity 'maps' the flow and transport is difficult to read at a small scale. Their modeling exercise, similar to their 2001 setup, demonstrated that they could accurately describe the heterogeneous soil structure but still not predict the large-scale transport parameters. Other experiments conducted with 3D structures of different particle-sized sand cubes show that predicting water flow at fine scales is very challenging, even under the most controlled conditions. Yoon (et al., 2008) found errors of nearly 10% when trying to predict the flow time of a paramagnetic tracer with magnetic resonance imaging (MRI) through a heterogeneous sand-cube mixture. Also, Papafotiou (et al., 2008) discovered the faults of two different methods, the Lattice-Boltzman and multi-step outflow methods, where neither could predict flow behavior in similar conditions. While the

aforementioned work relates to flow and transport rather than evaporation, it illustrates the role that capillary and film forces play in liquid motion, which in evaporation processes is evidenced by the complex dynamics of the drying front.

Kozack (et al., 2005(a)) performed a study in which the Brooks-Corey equations of soil hydraulic properties of 11 different textural classes were found to strongly correlate to the pore-size distribution index (λ). The purpose was to explore relationships between evaporation (E), transpiration (T), and λ across different soil types and scale E and T among the soils. Similarly, Kozack and Ahuja (2005(b)) studied the relationships between saturated hydraulic conductivity (K_s) and air-entry pressure head (ψ_b) and how they relate to infiltration and soil water contents during redistribution across soil textural classes. They found quantitative relationships between λ and evaporation as well as λ – dependence in infiltration and soil water storage relations that can be used to estimate infiltration and soil water contents across soil types for other soils and conditions by interpolation. These studies were conducted with the Root Zone Water Quality Model to simulate infiltration across 11 textural classes. While this study includes data from actual soil columns studied in a laboratory setting, much data has also been generated from the HYDRUS numerical modeler for evaporation rates and cumulative evaporation across combinations of soil textures.

Spatial heterogeneity contributes to the complexity of predicting the rate at which potentially hazardous chemicals produced by agricultural operations and other various industries move throughout the vadose zone. Quantitative descriptions of chemical transport on a field scale are necessary for the management of these chemicals to minimize groundwater pollution. Although it may be difficult to predict flow in a

heterogeneous media with laboratory samples and numerical modeling, to achieve this it is necessary to develop a more complete understanding of transport properties and evaporation of the vadose zone (Russo et al., 1998).

Flow across textural boundaries is further visualized by the colorfully illustrated study by Schaap (et al., 2008) in which 101 cubes of fine sand and 49 cubes of coarse sand cubes were imbibed with water and then allowed to drain. Water content was measured by neutron transmission tomography and boundary conditions were found to play a major role in the system that was designed to have continuous structures of media with different hydraulic properties. They showed that water dynamics depend on the spatial arrangement of the two materials and also that drainage was most efficient in structures of coarse sand that were connected to the top of the column even though it was covered with foil to minimize evaporation. Although Schaap's (et al., 2008) work focused on drainage, it further highlights the importance of textural boundaries in water motion. . Capillary force contrast between coarse and finer textures play a major role in water redistribution.

Combining the effects of textural boundaries and solute transport represents a basic element of vadose zone heterogeneity. In the realm of infiltration, as previously discussed, fuel spills and commercial underground storage leaks represent possible introductions of light nonaqueous-phase liquids (LNAPLs) that Schroth (et at., 1998) have shown to exhibit different flow patterns at varying saturation amounts. Their experiment involved a coarse-textured inclusion at an angle within a fine-textured matrix and observed the flow of water and LNAPLs. High saturation and low saturation alike showed the LNAPLs following the textural interface without intrusion into the fine while a moderate saturation

did result in intrusion into the coarse. The LNAPLs were able to penetrate the coarse when moderately saturated because the smaller pores of the fine were water-filled and the LNAPLs could move into the larger pores of the coarse intrusion. The Schroth (et al., 1998) study illustrates the complexity and importance of the combined effects of textural boundaries and solute transport. In the realm of evaporation processes, textural boundaries also play a very strong role on transport. Shokri et al. (2010) showed that a horizontal textural interface will result in different gradients and fluxes depending on texture placement. Placing a coarser texture above a finer one will result in "mulching" where the low air entry of the coarse creates an evaporation barrier but changing their positions will create a negative pressure gradient at the interface due to the finer texture's high air entry value. Their 2D sand experiments show a drying front receding into the fine texture until an air pathway reaches the coarse material and a "rapid and disproportionate water displacement" in the coarse ejects water to the upper fine layer.

Experiments dealing exclusively with coarse and fine textures and the pressure gradients that result from the complex relationships they form will now be discussed as they directly relate to this paper. Solute transport, especially salts, being of much importance in porous media is the focus of several more studies. Bechtold et al., (2011) conducted experiments in which a column was filled with a coarser sand in the inner core and a ring of finer sand around it and the location of surface salt deposition during evaporation was noted. Surprisingly, the area of greater evaporation, the fine surface, did not accumulate salt; it accumulated on the coarse surface instead. They proposed that preferential flow happens vertically and solute accumulation is not governed by evaporative fluxes but by, "*the relative differences of the hydraulic conductivities*, the scale of the heterogeneity,

and the diffusion coefficient and solubility of the dissolved substance." They defend this stating that once the salts reach the surface (via fine textures) molecular diffusion moves them toward the area of lower hydraulic conductivity, which in their case was the coarse sand, due to capillary pressure conditions.

Several other studies similar in nature had very different results. Nachshon (et al., 2011(a)) found that salt accumulation in a similarly constructed heterogeneous porous media resulted most of the salt accumulating in the fine pores, not the coarse pores. This salt accumulation in the fine media decreased the evaporation rate because the salt essentially blocked pores and blanketed the surface. The coarser media continued to evaporation but its rate was limited by vapor diffusion. In addition to a preferential deposition of salt crusts over the fine textures, Nachshon et al., (2011(b)) established an increase in salt precipitation along the textural interface also. Nachshon (a) took place with a receding water table and Nachshon (b) took place with a constant hydraulic head and both experiments still showed similar results.

The idea of salt accumulation in a heterogeneous combination of texturally contrasting media arose from the discovery of an evaporation phenomenon where the combination of two different textures produced higher cumulative evaporation amounts than either texture could produce on its own and will now be referred to as "Evaporation Synergy". Or et al., (2007) conducted experiments in which a coarse textured sand and fine textured sand were placed adjacent each other in a column. The system was initially saturated and results showed an earlier drying front propagating in the coarse media while the fine remained saturated. They compared the drying process to that of a pair of different sized capillaries where water flows from the receding meniscus of the larger capillary to

supply the evaporating surface of the fine capillary. This means that not only is there a vertical pressure gradient established between the atmosphere and the evaporating surface of the porous media, but a lateral pressure gradient established between the coarse and fine media when the coarse hits air entry value and the atmosphere is still pulling upwards from the saturated fine media.

Lehmann and Or (2009) further explained the mechanisms behind the lateral flux between coarse and fine media by performing similar sand-in-column experiments. They claim the lateral gradient is due to the difference between the air entry value of the coarse domain and the minimum capillary pressure in fine textured region. With any porous media, the fine in this case, maintaining a higher capillary pressure gradient than gravitational and viscous forces is necessary for Stage 1 evaporation. They too found higher evaporation rates in heterogeneous columns than in their homogeneous counterparts.

Shahraeeni and Or (2010), and Shahraeeni (2011), attempted to quantify the proportion of water that evaporated from the fine and coarse portions by taking advantage of the suppression of surface temperature during the evaporation process using Infrared Thermography, confirming the conceptual model and the lateral transfer of water after the coarse had reached air entry value.

Much of the aforementioned work on evaporation from heterogeneous media was performed using sand textures. This study focuses on soil textures rather than sands, and as will be discussed later, the role of viscous forces in soils is more important than in sands, as stated inOr et al., (2007) that viscous limitations in the fine may be more prevalent if the fine is composed of clay-sized particles instead of relatively small sand-sized particles. The lower viscous drag is due to more rounded

shaped and larger pores that result in less tortuosity within the medium. In addition, pore shape is important in liquid-film transport (Pillai et al., 2009), which as mentioned is also an important component of the evaporation mechanism.

3. Materials and Methods: Project Description

Evaporation synergy has not been studied previously in finer soil media, with previous studies limited to relatively coarse and fine sands. Although the mechanisms that cause this phenomenon should be present in finer media, it is found here that they do not necessarily result in evaporation synergy. Within the 12 classified soil textures, the porous media properties of hydraulic conductivity ($K(\theta)$) and Moisture Characteristics exhibit a much greater range than in sands. Indeed, as presented in this manuscript, the resulting evaporation process for soil media was found to be much more complex, with the presence of vertical and lateral pressure gradients resulting in either evaporation synergy or suppression. This study addresses the criteria in order for evaporation synergy to occur in all combinations of the 12 soil textures.

The purpose of this study was to determine which of the 66 combinations of soil textures would exhibit evaporation synergy and to develop a conceptual model to explain the necessary criteria to achieve synergy. Evaporation from all heterogeneous and homogeneous soil textures was investigated numerically using the HYDRUS numerical modeler to determine evaporation rates and cumulative evaporation amounts. Furthermore, two combinations of soils were selected based on the numerical results and investigated in the laboratory after construction of physical models. The two pairs were selected to represent one

combination that exhibited evaporation synergy and one that did not show synergy characteristics within the numerical models. In addition, the same coarse texture was used for the two pairs to reduce the number of unknowns to assist in identifying the key controlling mechanism.

This study furthers the understanding of the criteria necessary for evaporation synergy to occur within a bi-textured soil system. Because the previous studies involve well sorted sand, key simplifications were made to the equations that quantify the mechanisms within them. The Lehmann et al. (2008) study of heterogeneous mixtures of sand introduced a characteristic length (L_{cap}) that determines conditions for the transition between stage 1 and stage 2 evaporation. However, while the value of L_{cap} depends on air entry and liquid viscosity, viscous dissipation in sand can easily be neglected, which it was in these studies. Later, Nachshon (2011a) generated an equation based on the Lehmann et al. (2008) work to predict the time duration of S1 evaporation (t_{S1}) also for sand:

$$t_{S1} \approx L_{cap}(A_{coarse}+A_{fine})\Phi/(e_o A_{fine}) \qquad \text{Eq. 1}$$

where L_{cap} is a function of the largest and smallest capillary radii, A is the cross-sectional area of the evaporating surface (m^2), e_o (m^3/m^2 d) is the potential evaporation rate, and Φ is the porosity. Because both Lehmann et al. (2008) and Nachshon (2011a) both ignored the role of viscous forces on L_{cap} it was found in this study that their equations do not predict evaporation results for finer soils, where viscous forces are important and may even dominate hydraulic characteristics. A better understanding of the criteria controlling enhanced or suppressed evaporation within a bi-textured soil system is necessary.

3.1   Technical Background on Evaporation Synergy

Evaporation Synergy is a phenomenon that is the result of several mechanisms that combine with various porous medium properties whereby a heterogeneous soil-pair experiences higher cumulative evaporative losses than either texture on its own. The process of evaporation is here described for a bi-texture system that begins saturated and has no flow boundary along the bottom. Coarse and fine textures are distinguished by the coarse having a lower air-entry value (h_b) and a higher saturated hydraulic conductivity (K_{sat}). In cases where both have similar air-entry values, the coarse is defined as the one with the higher K_{sat} value.The first phase of this process is evaporation from a completely saturated system which proceeds at the potential evaporation rate. As water leaves the system, water tension increases within both media. The major change in this process happens when soil-water tension within the coarse texture reaches air-entry value (h_b), the hydraulic conductivity of the near surface coarse texture begins to decrease and its saturated front begins to recede below the surface. At this point, both the coarse and fine are both still hydraulically connected to the surface and the evaporation rate is sustained at e_o. The second phase of this process begins when the coarse soil's water tension reaches its "critical value" and the films sever from the soil surface: evaporation rate from the coarse media decreases since it is now limited to vapor diffusion from a subsurface evaporation front. The fine media, however, is still hydraulically connected to the evaporating surface because its air-entry value is much higher. The difference in air-entry value between coarse and fine was defined by (Lehmann and Or, 2009) as a difference in the driving capillary force (Δh_{cap}) (Eq 2),

$$\Delta h_{cap}=h_b{}^f-h_b{}^c$$ Eq. 2

This difference in capillary force between the two media causes a lateral pressure gradient across the boundary separating the two textures. This horizontal pressure gradient drives from the coarse towards the fine, which the fine then transports upward toward the surface of the fine for evaporation: the upward transport is drivenby the vertical pressure gradient that is generated by the evaporation process. The fine continues to pull water from the coarse until the combination of capillary and viscous dissipation exceed the 'critical value (h_r)" of the fine media. At that moment, the fine media becomes hydraulically disconnected, it enters Stage 2, and the S1 stage for the entire system ends.

If only this mechanism of pressure difference was sufficient to determine evaporative behavior then every combination of a bi-textured system would exhibit evaporation synergy. In every case, the difference in air-entry values would create the vertical and lateral pressure gradients. However, there are other parameters important to the evaporation property that are controlled by porous medium properties, critically important for this process is the particle size distribution. At the large end, particle size determines air-entry value and it will be lower in a texture with larger particles. At the small end, particle size determines the h_r for film rupture, and also the maximum capillary depth from which moisture can be drawn. Particle size distribution also determines the unsaturated hydraulic conductivity function ($K(h)$) of the porous medium. For the coarse media $K(h)$ reflects the amount of viscous dissipation that the fine media has to overcome to extract water laterally from the coarse media. For the fine media, $K(h)$ controls the gradient necessary to get sufficient moisture to the evaporation surface to sustain S1. These are important properties because evaporation synergy does not solely depend on the pressure gradients to pull water laterally and vertically. The fine must possess a

hydraulic conductivity (K(h)) swift enough for water to travel to its surface before it becomes hydraulically disconnected at critical value. These conditions must be met within the fine to allow a flux that meets the evaporative demand (e_o) (Eq 3).

$$Q^{fine} \geq E^f_{rate} \qquad \text{Eq. 3}$$

Similarly, the porous medium properties of the coarse cannot be ignored. Even though the capillarity of the fine may be able to supply a negative pressure gradient on the coarse it may not be sufficient to overcome the viscous forces created by the capillarity of the coarse. Simply put, if the coarse is not coarse enough it will not lose enough water to the fine to sustain its demand.

This conceptual model of the intricacies of evaporation synergy demonstrates how multiple factors work together or against each other in a bi-textured system. It is necessary for certain criteria to be met in order for evaporation synergy to occur. The two textures must exhibit different air-entry values to create the lateral and vertical pressure gradients, the fine must possess a swift enough hydraulic conductivity to allow water to move to its surface before it reaches its own critical value, and finally the viscous forces within the coarse must be low enough for water to be pulled from itself to the fine. These are the conditions necessary for evaporation synergy to occur.

Other researchers have succeeded in determining the duration of stage 1 (t_{S1}) and the evaporative depth (L_{S1}) at t_{S1} in heterogeneous fine and coarse sands (Nachshon *et al*, 2011(a) and Lehmann *et al*, 2008, respectively). The quantitative methods are based on the difference in capillary forces between the fine and the coarse (Δh_{cap}), which Lehmann (*et al*, 2008) refers to as a characteristic length (L_C). L_c is calculated with the potential evaporation rate (e_0), hydraulic conductivity (K(h)), and the

characteristic gravity length (L$_G$), and is the length at which the gravitational head difference (Δh$_G$) balances the maximum capillary driving force (Δh$_{cap}$) causing cessation of flow.

$$L_C = \frac{L_G}{1+\frac{e_0}{K(\Theta)}}$$ Eq. 4

Lehmann (*et al*, 2008) also quantified the value of L$_G$ from an individual soil's empirical constants by linearizing the moisture characteristic curve. Their equation expresses L$_G$ as a function of vanGenuchten parameters: α (approximately equal to the inverse of the air-entry value) and (n) approximately a measure of the pore-size distribution (vanGenuchten, 1980).

$$L_G = \frac{1}{\alpha(n-1)} \left(\frac{2n-1}{n}\right)^{\frac{2n-1}{n}} \left(\frac{n-1}{n}\right)^{\frac{1-n}{n}}$$ Eq. 5

Furthermore, Eq 6 predicts a length defined by viscous dissipation (L$_V$), which represents the resistance to capillary forces and can be determined by the relationship:

$$L_V = \frac{K(\Theta)}{e_0} * L_C$$ Eq. 6

Note that the higher the potential evaporation rate, the shorter the maximum depth of the saturated front before transition to stage 2, as suggested by Phillip (1957). It is worthy of note that the authors of Lehmann *et al* 2008 did take viscous forces into consideration while developing predictive equations for the different porous media characteristic lengths. This is evident by the rearrangement of variables to display a quantitative relationship between the three forces.

$$L_C = \frac{L_G}{\frac{L_G}{L_V}+1}$$ Eq. 7

However, because their interest was to apply this equation to coarse media (as per their experiments), this condition is only valid "as long as the gravitational length L$_G$ is much shorter than the length defined by the

viscous dissipation L_V." The authors go on to mention "the role of viscous dissipation would undoubtedly become important for evaporation from fine-textured media at which the viscous length could become limiting before the gravitational length."

Also, these equations were developed with a linearization of the water retention curve for water saturation as a function of capillary head. A tangential line was drawn from the inflection point along the curve to determine Δh_{cap} (at the intersection of the tangent line and the saturated moisture content value), and L_G at the intersection of the tangent line and the y-axis), which were then used to form the relationships in the equations above. This method may suffice with sands where the range of capillary head is small but soils possess a much wider distribution of pore-sizes, which is why the capillary head is usually graphed on a log-scale for soils. It may be more appropriate to use a log-linear relationship between capillary head and water saturation for soils and, although this exercise is left for future investigations, it could explain why these equations do not accurately predict the characteristic lengths of finer-textured soils.

Lehmann (*et al*, 2008) went on to estimate the evaporative depth at t_{S1} using the gravitational length and other porous media properties:

$$t_{S1} Depth \approx (\varPhi - \theta_r)L_G \qquad \text{Eq. 8}$$

Expanding upon the methods from Lehmann (*et al*, 2008), Nachshon (*et al*, 2011(a)) developed an equation based on their L_C equations to predict the t_{S1} for a bi-textured system:

$$t_{S1} \approx \frac{L_C(A_C+A_F)\varPhi}{e_0*A_F} \qquad \text{Eq. 9}$$

where A_C and A_F are the surface areas of the coarse and fine, respectively, and $\varPhi$ is porosity.

Equations 4-9 are all derived from linear head and saturation relationships that would not accurately represent a finer soil. The equations

also do not account for viscous forces within finer soils that would interfere with the L_G and L_C relationships. For these reasons, these equations do not and should not be expected to accurately predict characteristic lengths or t_{S1} for finer soils and deriving new equations for soil is necessary.

3.2   Materials and Methods

The evaporation process was investigated both using laboratory experiments and by numerical methods. The numerical work generated the majority of the data presented in this paper, and provided the core of the information used to test the theoretical understanding.

The laboratory experiments were not designed to test the synergy hypothesis but rather designed as a demonstration of the phenomenon that was more thoroughly investigated by the numerical work. Two bi-textures were selected to demonstrate synergy and non-synergy cases. The following two sections describe in detail the methods used for the laboratory experiments and the numerical investigation.

3.2.A   Materials and Methods used for Laboratory Investigation

For each bi-texture pair tested, four columns were placed into an evaporation chamber. One column was filled the bi-texture, the second and third columns were filled with a homogeneous version of the fine or coarse media used for the bi-texture and the fourth column was filled with DI water to measure the potential evaporation of the chamber. All soil columns were saturated with DI water, and placed on mass balances inside an evaporation chamber to measure the mass of moisture lost from each. The mass balances were connected to a laptop for data collection.

Chamber design. To control the relative humidity within the evaporation chamber, four small cages where placed equidistant from the columns, each containing approximately 90-100 g of calcium chloride beads. The dehydration beads draw chamber moisture and sustain a constant vapor. By this method the potential evaporation rate at was sustained at approximately 0.4 cm/day within the chamber. Damp Rid brand dry beads were used in the Synergy Experiment run and Dri-z-air brand dry beads were used in the Non-synergy Experiment run, the difference in brand was for no other reason than availability. Both brands contained calcium chloride as the desiccation agent. The evaporation chamber was constructed using Plexiglas. To facilitate taller columns, the original evaporation chamber's height was increased with greenhouse plastic that was laid over wooden poles secured to the walls of the chamber. The chamber stood 90 cm tall, 100 cm long, and 60 cm deep. The four mass balances and columns stood 20 cm from either wall and 20 cm from each other. The surface of the columns were 40 cm from the top of the evaporation chamber (greenhouse plastic.) For both the Synergy and Non-synergy runs three of the columns contained different soil media while a fourth column, filled with deionized water, was used as a Water Blank to provide the value of potential evaporation rate. Because of room constraints, both sets of experiments, synergy and non-synergy were not run concurrently. The synergy experiment was run first, and then the non-synergy experiment was run. Unfortunately, there were a few difficulties with the experiments. (1) The water level of the blank in the Synergy Experiment run was allowed to fall down to 10.3 cm over the course of the experiment, resulting in an apparent decreasing potential evaporation rate as the experiment progressed. The problem was corrected before the non-synergy experiment was started. The water level at the top of the column in

the Non-synergy Experiment run was maintained by a Mariotte Bottle System to sustain the water level in the column as water evaporated from its surface. Both the evaporation column and the Mariotte Bottle where placed together on the same mass balance to avoid friction within the delivery system, and barometric pressure variations from affecting the mass loss data.

Selection of soils. For the setup designed to demonstrate Evaporation Synergy, one column contained homogeneous Loamy Sand, one contained a homogeneous Silt Loam, and one contained a heterogeneous combination of Loamy Sand and Silt Loam. For the setup designed to demonstrate Non-synergy Evaporation, one column contained homogeneous Loamy Sand, one contained homogeneous Sandy Clay, and one contained a heterogeneous Loamy Sand and Sand Clay. The heterogeneous columns did not consist of two mixed soil media, but two media kept separate and sharing a common vertical boundary between the two.

Column construction. The methods used to pack the soil columns varied depending on packing difficulty and wetting-up difficulty. Two methods were used to build the columns for the Synergy Experiment. For the bi-textured Loamy Sand/Silt Loam soil and homogeneous Silt Loam soil, a 44 cm tall x 6 cm diameter (1 L) glass-graduated cylinder was packed with soil media while a glass tube (7 mm in diameter) was held vertically along the wall from base to surface with several cm of excess protruding from the top. After the soil had been packed, water was slowly added to the glass tube to allow the soil to slowly "wet up" by capillarity.

The second method, used for the homogeneous Loamy Sand soil and the homogeneous Silt Loam soil, involved connecting three sections of PVC pipe connected by electrical tape to seal the pieces together to equal

the total height of the 1 L glass-graduated cylinders. These were wetted up by a hanging Erlenmeyer flask attached to a sealed opening in the bottom of the PVC column. Similar to the graduated cylinder method, the PCV columns were slowly wetted up by capillarity by raising the Erlenmeyer flask as water climbed higher in the columns. The PVC columns were the same dimensions as the glass graduated cylinders. It was thought that this method would make it easier to pack the vertically oriented heterogeneity.

All columns, PVC and glass alike, except the homogeneous Sandy Clay were filled with oven-dried soil and firmly packed with every 2-3 cm of added soil. The soils in the heterogeneous columns were kept separate during filling by a thin piece of cardboard wrapped with duct tape just wide enough to span the diameter of the graduated cylinders and prevent the textures from crossing over the boundary. It became apparent that the homogeneous Sandy Clay was too hydrophobic in its dry form to allow water to imbibe by capillarity. To overcome this difficulty, different measures were taken to saturate it. The most successful method, that prevented layering and separation of clay and sand components, was approached as follows. The Sandy Clay was wetted and kneaded like dough until it was the texture of oatmeal. This kept the two particle sizes well mixed and prevented settling which would occur with any of the other filling methods. Once it had reached the point of becoming "shiny" as opposed to "sticky" it was added in golf ball sized clumps to the graduated glass cylinder and patted down and agitated to encourage settling with a solid rod of plexiglass.

Building the soil textures. The Sandy Clay is simply composed of a half-and-half mixture of laboratory grade Kaolinite clay powder and 12-20 Accusand. The Silt Loam was collected in the Willamette Valley in Oregon then dried and classified as 32% sand, 57% silt, and 11% clay. The Loamy

Sand was collected and classified (originally 2781 g as a Sandy Loam at Sand 70% Silt 13% Clay 17%) then amended with 1500 g of 12-20 Accusand to achieve a Loamy Sand texture of 81% sand, 8% silt, and 11% clay.

Data Collection. LabView was used to write a data collection program. The data was collected by monitoring the 4 Mettler Toledo New Classic MF mass balances for the amount of water lost from each column. Every 10 minutes the program updated a text file with the mass of each column. From this data the mass vs. time, cumulative evaporation vs. time, and evaporation rate vs. time graphs were generated.

Numerical Models

3.2.B   Materials and Methods used for Numerical Investigation

The HYDRUS 2D program was selected to model the soil water evaporation dynamics of the experiments. "HYDRUS is a Microsoft Windows based modeling environment for the analysis of water flow and solute transport in variably saturated porous media. The software package includes computational finite element models for simulating the two- and three-dimensional movement of water, heat, and multiple solutes in variably saturated media. The model includes a parameter optimization algorithm for inverse estimation of a variety of soil hydraulic and/or solute transport parameters. The model is supported by an interactive graphics-based interface for data preprocessing, generation of structured and unstructured finite element mesh, and graphic presentation of the results" (PC-Progress 2008).

The program has a wide range of uses (Roberts et al., 2009, Kandelous et al., 2011, Starr et al., 2005) and variability is minimal as long

as the models are properly scaled to the experiments (Abassi et al., 2003). The HYDRUS graphical user interface (GUI) allowed for easy selection of soil textures and initial and boundary conditions for the numerical models. Soil properties were represented using the vanGenuchten parameters for the specified soil texture and hydraulic properties.

The numerical models were conducted in 2D instead of 3D and model domain was matched to the size of the columns used in the laboratory experiments. The numerical experiments were run to identify the *relative* amounts of evaporation from the soil columns rather than the *quantitative* amounts, as only the presence or absence of evaporation synergy was the main aspect of this study. Therefore, the actual amount of water lost to evaporation from the soil columns was not crucial. It is important to note that the size of the domain is not expected to affect the occurrence of synergy, as long as the depth of the columns are greater than L_{cap}. That said, the size of the domain and the relative proportion of coarse and fine texture will affect the quantity of moisture lost during synergy. Mimicking the experimental procedure, the model soils were initially saturated and allowed to dry over a period of at least 30 days at constant evaporation rate (diurnal variability was not modeled either experimentally or numerically). The model dimensions were 2D and rectangular and the columns were set to a height of 40 cm and width of 6 cm. The vertical discretization was set to a count of 88 and horizontal discretization at 11 (making the column 10 nodes across and 87 elements from top to bottom.) To make the nodes five times tighter at the surface the RS1 was set to 1 and RS2 was set to 5. The initial conditions for every model were completely saturated with a transpiration rate of 0 cm/day and an evaporation rate of 0.4 cm/day to reflect conditions of the physical models. Critical value for all model soils were 10,000 meters and

hysteresis was included in the retention curve that was set to the initially drying curve. Only the top of the columns were open to the atmosphere while the bottom and sides of the columns had no flow boundaries. This was to examine the effect of evaporation without drainage. Data print times for all models were set coarsely, initially, to determine the duration of stage 1 evaporation. Then, a tighter print-time interval (approximately 10x more readings) was applied around the t_{S1} to get a more precise stage 1 duration. Each model was run for a period of 60 days.

4.   Results

4.1   Results from Numerical Investigation

Individual textures possess different characteristics that result in different evaporation rates and evaporation amounts. The numerical model HYDRUS was used to determine the duration of the first stage of evaporation. Soil textures where represented using the vanGenuchten parameters for soil-water retention (vanGenuchten, 1980.) To clarify terminology used, the coarse texture in a pair is always the one with the highest value of air-entry pressure (h_b). Note that there is not a direct relationship between h_b or K_{Sat} and Stage 1 duration (t_{S1}). For instance, the homogeneous textures silt and clay show very different durations of first-stage evaporation, 8.78 days and 0.96 days respectively, although their saturated conductivities are very similar, 0.25 cm/hr and 0.20 cm/hr. Soil textural parameters (aka, vanGenuchten parameters), saturated conductivity and duration of Stage 1 evaporation are shown on Table 1.

When the homogeneous textures are placed together so they share a common vertical boundary the resulting evaporative loss from the bi-

texture system is not the average of the two media. While it may appear counterintuitive at first, the two media interact to create a new system with a unique evaporation process that may result in evaporative synergy. Of the 66 heterogeneous combinations tested, 20 exhibit evaporation synergy (Figure 1), where the combined cumulative evaporation is greater than either homogeneous texture can produce on its own. The remaining 46 bi-texture combinations exhibited cumulative evaporation losses that were in between the homogeneous textures, but not necessarily the average of the two. In some cases, the non-synergistic pair showed slight "enhanced" evaporation where the cumulative losses were slightly higher than the average of the homogeneous losses.

Table 1. Soil textural and hydraulic parameters associated with the vanGenuchten equations for moisture retention and hydraulic conductivity. The t_{S1} lists the duration of the first stage (constant stage) of evaporation obtained from the numerical model results.

| Texture	Ks (cm/hr)	α (1/cm)	N	θr	θs	M	t_{S1} (days)
Sandy loam	4.42	0.075	1.89	0.065	0.41	0.47	10.73
Loam	1.04	0.036	1.56	0.078	0.43	0.36	10.68
Silt Loam	0.45	0.02	1.41	0.067	0.45	0.29	10.26
Loamy sand	14.59	0.124	2.29	0.057	0.41	0.56	9.25
Sand	29.7	0.145	2.68	0.045	0.43	0.63	9.00
Silt	0.25	0.016	1.37	0.034	0.46	0.27	8.78
Sandy clay loam	1.31	0.059	1.48	0.100	0.39	0.32	5.95
Clay loam	0.26	0.019	1.31	0.095	0.41	0.24	4.73
Silty clay loam	0.07	0.01	1.23	0.089	0.43	0.19	2.36
Sandy clay	0.12	0.027	1.23	0.100	0.38	0.19	1.38
Clay	0.2	0.008	1.09	0.068	0.38	0.08	0.96
Silty clay	0.02	0.005	1.09	0.070	0.36	0.08	0.24
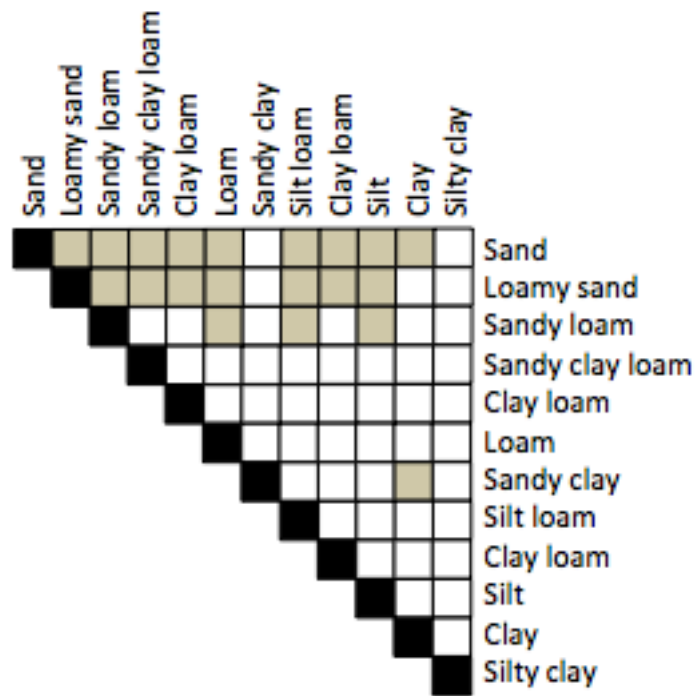
Figure 1. Combinations of bi-textures that synergized (beige) and those that did not (white).

There were some general characteristics of soil properties for the synergizing pairs. The bi-textures that did exhibit synergy (Figure 1) all contained one of the textures in the pair that was either Sand, Loamy Sand, or Sandy Loam, except for one combination, the Sandy Clay and Clay. This shows that synergy requires a relatively coarse and a relatively fine portion to perform synergy. It is also worthy to note that the one exception, Sandy Clay with Clay, synergized although both had high air entry values and low saturated hydraulic conductivities, indicating the sensitivity of the criteria necessary for synergy to occur and the complexity of the mechanism involved.

The anatomy of the evaporation rate curve for synergy cases shows the following characteristic features. The first stage of evaporation (S1) is

multi-stepped (Figure 4). The length of time to the first step is shorter than the S1 duration of either homogeneous media, and the duration of the last step is far longer than the S1 duration for either homogeneous media. It is the length of time between the end of the homogeneous S1 and the end of the heterogeneous S1 that provides the extra water loss causing synergy. Once the system enters S2, the rate plummets similarly to the homogeneous cases and third stage seems to be unaffected, although the third stage was not the focus of this study. The timing and duration of each individual 'step' in the heterogeneous-S1 evaporation process are listed in Appendix 1 for all synergizing bi-textures. However, as will be noted later, the exact duration of each 'step' depends on the scale of the problem.

In every bi-textured combination it was found that

$$t_{S1}{}^c < t_{S1}{}^f \qquad \text{Eq. 10}$$

where the stage 1 duration of the finer texture (e.g., 29 days for Silt Loam in Figure 4) was greater than the stage 1 duration of the coarse texture (e.g., 21 days for Loamy Sand in Figure 4). Note that the superscripts in equation 9 refer to texture: c for coarse and f for fine. Recall that, the term 'coarse' is used for the texture with the higher air-entry value (h_b). This means that the coarse (Loamy Sand) transitions into stage 2 evaporation first (e.g., 7 days in Figure 4). The fine (Silt Loam) continues evaporating at the S1 stage (evaporation front located at the soil surface) throughout all of the step-wise decreases in evaporation rate (7, 10, 11, and 21 days, Figure 4) (described later as t_{Step} found in Table 2) until the fine texture finally transitioned into stage 2 evaporation marking the last step of the first stage of evaporation for the system (e.g., 29 days in Figure 4). The longer t_{S1} duration sustained by the finer texture is a necessary condition of evaporation synergy. Without the prolonged S1 the system would plunge into a vapor diffusion controlled evaporation state where enhanced

evaporation rates would not be possible due to a lack of film connections connecting the receding wetted front to the soil surface.

The anatomy of the evaporation rate curve for non-synergy cases shows the following characteristic features (Fig. 6). The first stage of evaporation (S1) is multi-stepped, but the system plunges into S2 (e.g., 8 days in Fig. 6) at a time that is intermediate between the homogeneous coarse and fine t_{S1}: e.g., 29 days for Silt Loam in Fig. 4, and 7 days for Loamy Sand in Fig. 6. In other words, the duration of the entire first stage is somewhere in between the homogeneous fine and coarse t_{S1} durations and drops into S2 evaporation without exceeding the evaporation rate of the fine media. The time of each individual 'step' in the S1 evaporation process for the non-synergy cases are also listed in Appendix 1.

Two bi-textures, one that the numerical model showed synergized and one that did not synergize, were selected to be tested in the laboratory. These were selected because in the numerical simulations the evaporation rate curve morphology evidenced very clearly the features detailed in the previous two paragraphs. These two bi-textures are also used as representatives for the discussion of the results from the numerical simulations, and their behavior is here described in detail. The hydraulic properties of the three textures comprising the two representative bi-textures are shown in Figures 2 and 3.

Numerical results. The Loamy Sand & Silt Loam combination developed synergy. Conversely, the Loamy Sand & Sandy Clay combination resulted in evaporation rates that are near the average of the two homogeneous components, a rather unexceptional behavior. The synergistic combination (Loamy Sand & Silt Loam) had a cumulative evaporation loss of 70 cm (at 60 days), exceeding the homogeneous Silt Loam at 55 cm after 60 days, by 21%. The non-synergistic bi-textured combination (Loamy Sand &

Sandy Clay) lost 41.5 cm of water, which is in between (although not the average) of the losses from the homogeneous Loamy Sand at 55 cm and Sandy Clay at 20 cm of water lost to evaporation. These two different textural combinations demonstrate the effect on cumulative evaporation of the evaporation synergy and non-synergy phenomena. It should be added, and will be discussed in detail later, that the specific amount of increase in the evaporation loss for a synergy case depends on the scale of the heterogeneity.

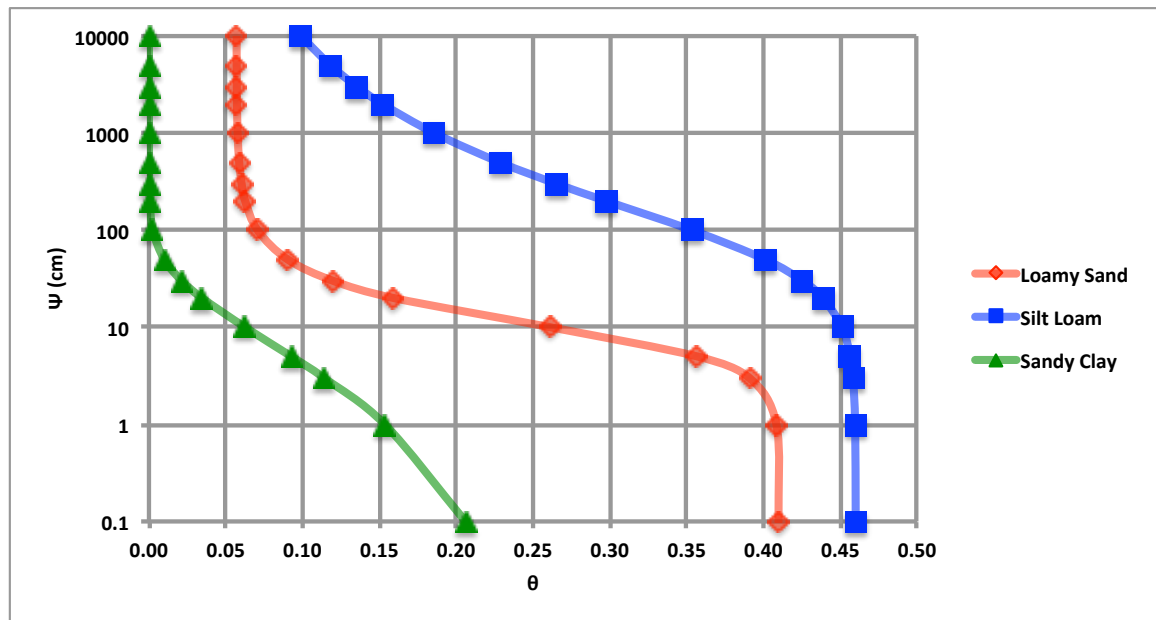**Figure 2**. Graph of matric potential (ψ) vs. moisture content (θ) for the three homogeneous textures that were used in the numerical and laboratory experiments. The curves were generated using the vanGenuchten equation (vanGenuchten, 1980).

Figure 3. Graph of hydraulic conductivity (K(ψ)) vs. matric potential (ψ) for the three homogeneous textures that were used in the numerical and laboratory experiments. The curves were generated using the vanGenuchten equation (vanGenuchten, 1980).
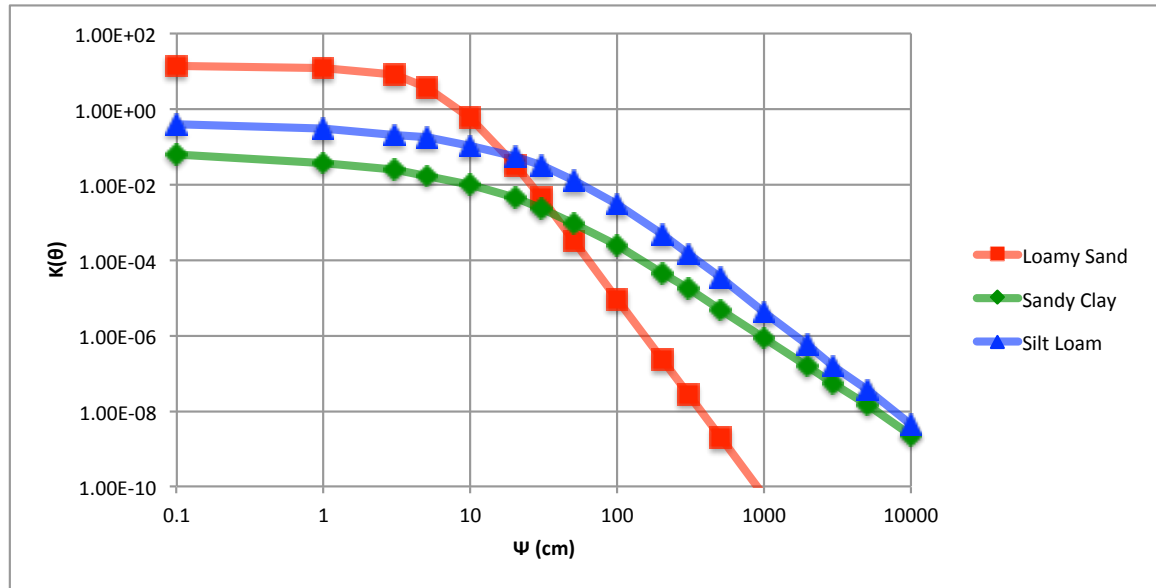
Figure 4. Results of HYDRUS simulation. Time evolution of the evaporation rate of the synergizing bi-texture comprised of Loamy Sand & Silt Loam and of its homogeneous counterparts.

Figure 5. Results of HYDRUS simulation. Time evolution of the cumulative evaporative loss of the synergizing bi-texture comprised of Loamy Sand & Silt Loam and of its homogeneous counterparts.

Figure 6. Results of HYDRUS simulation. Time evolution of the evaporation rate of the non-synergizing bi-texture comprised of Loamy Sand & Sandy Clay and of its homogeneous counterparts.
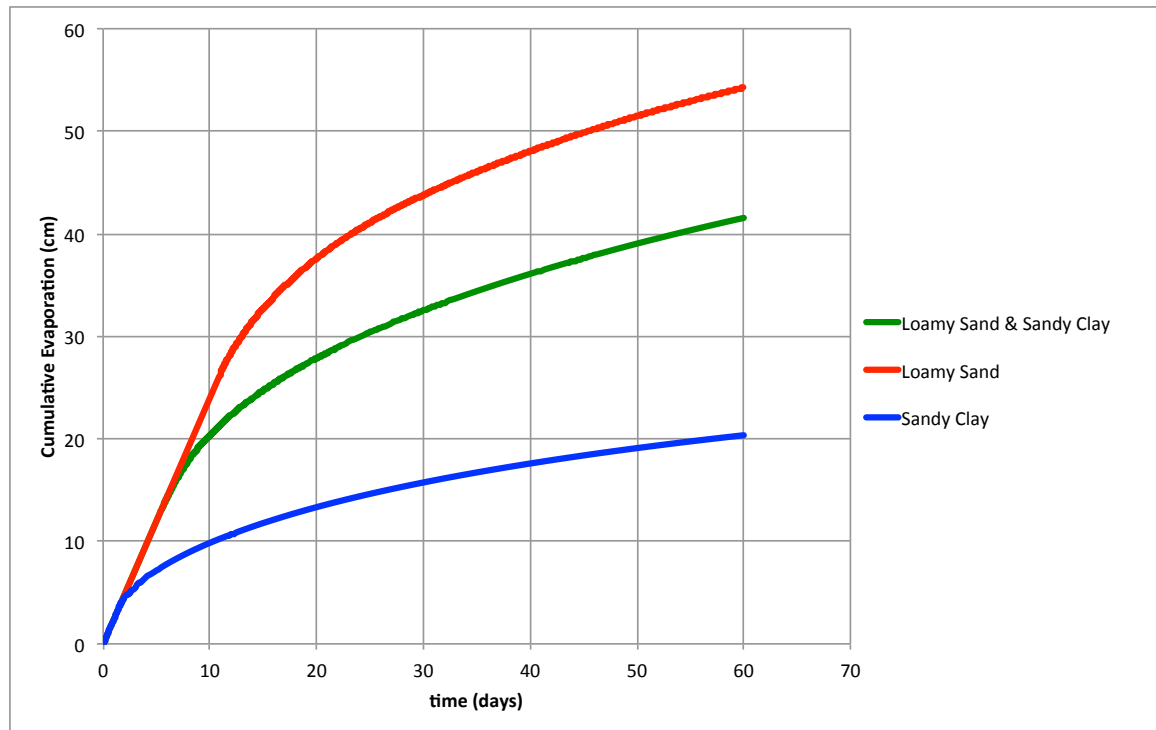
Figure 7. Results of HYDRUS simulation. Time evolution of the cumulative evaporative loss of the non-synergizing bi-texture comprised of Loamy Sand & Sandy Clay and of its homogeneous counterparts.
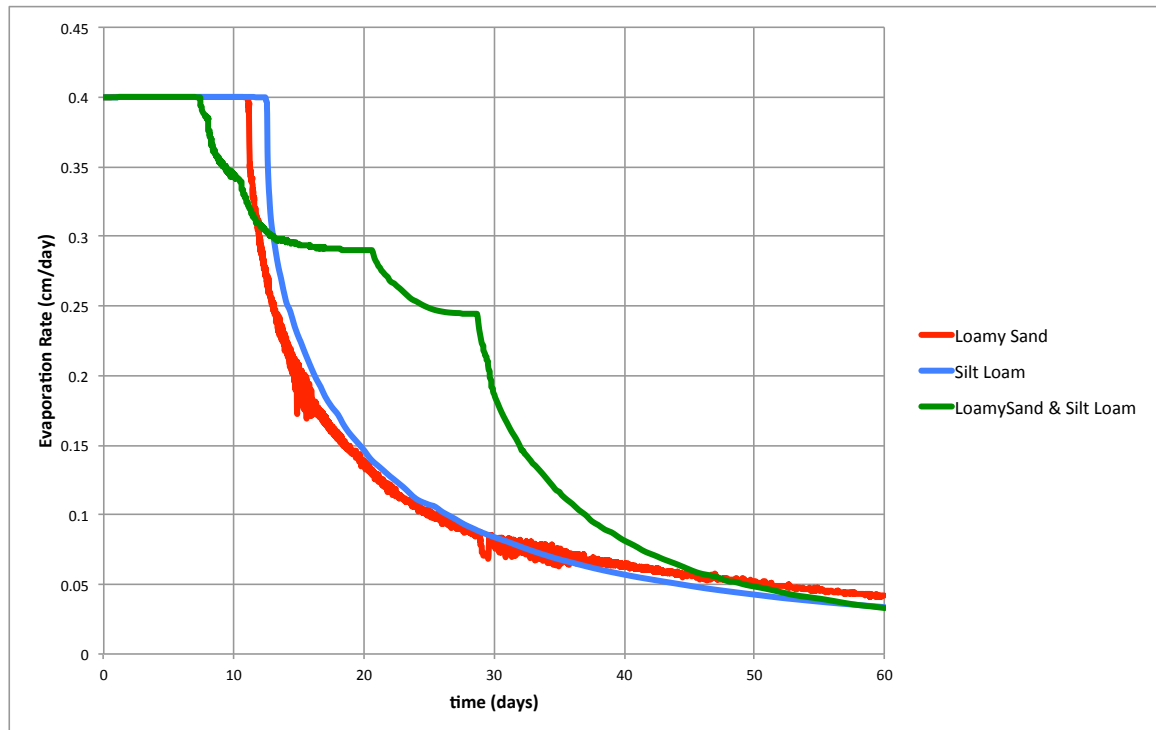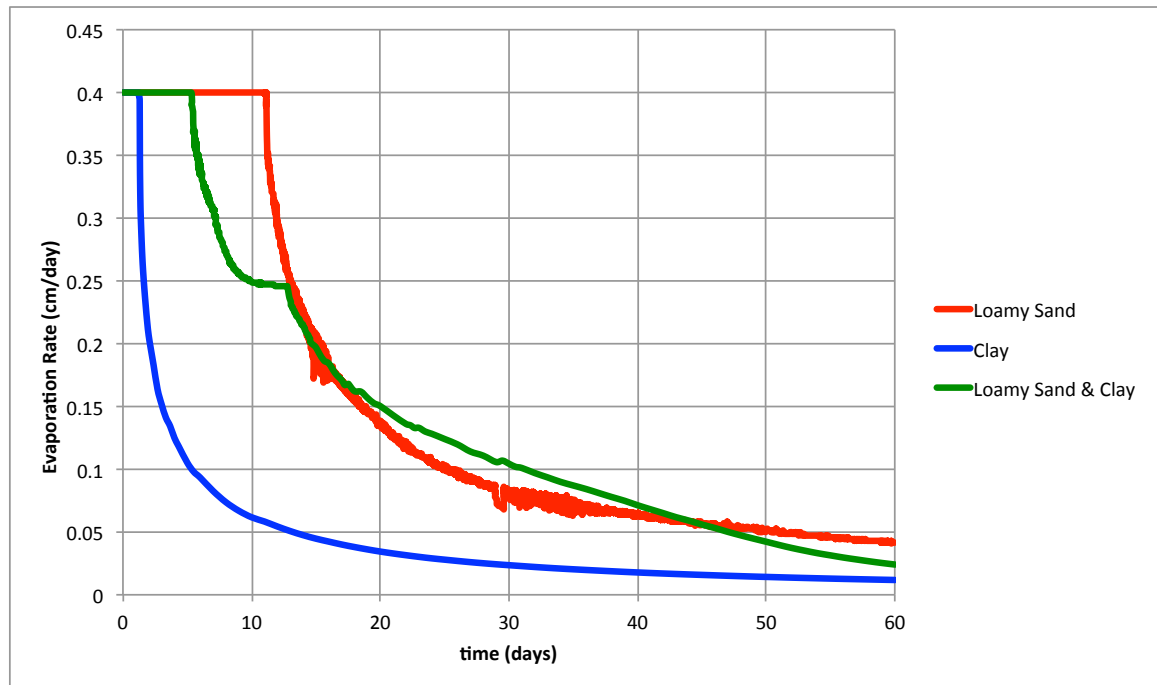
Figure 8: Results of HYDRUS simulation. Time evolution of the evaporation Rate of the non-synergizing bi-texture comprised of Loamy Sand & Clay and of its homogeneous counterparts.
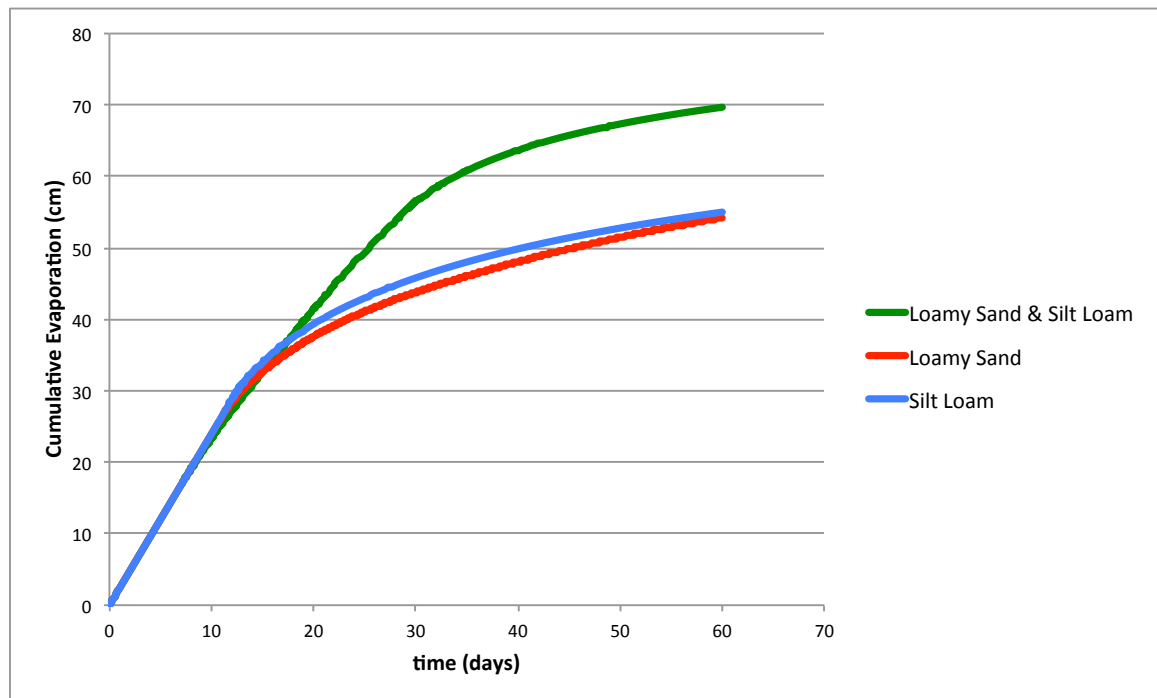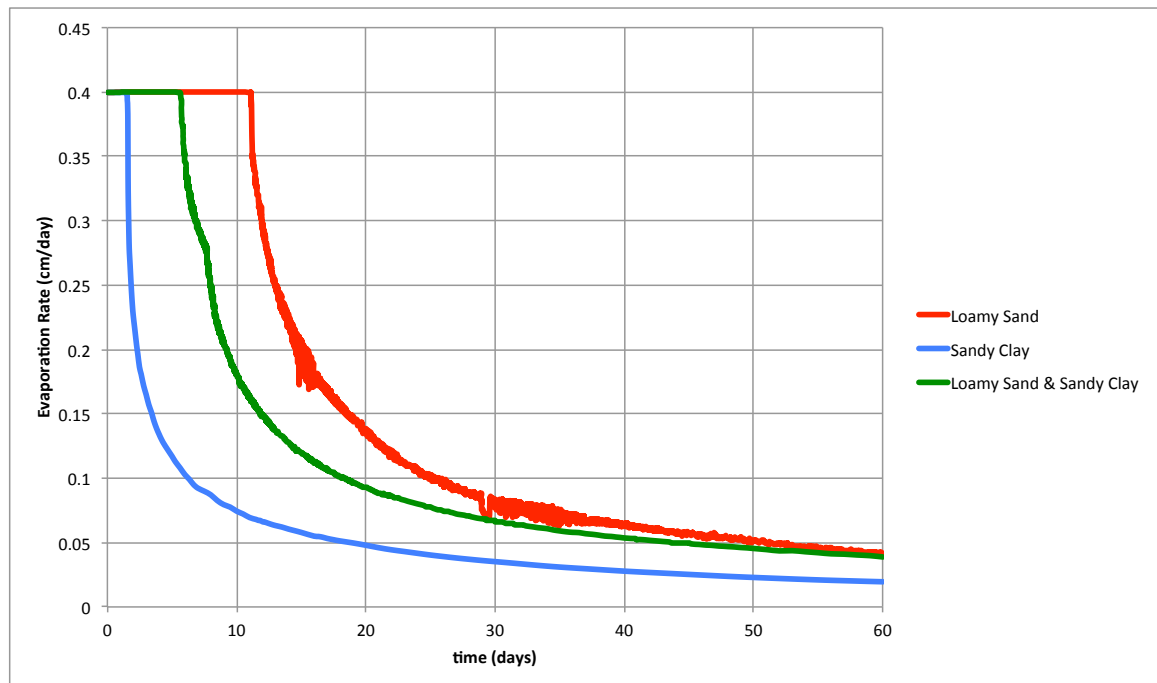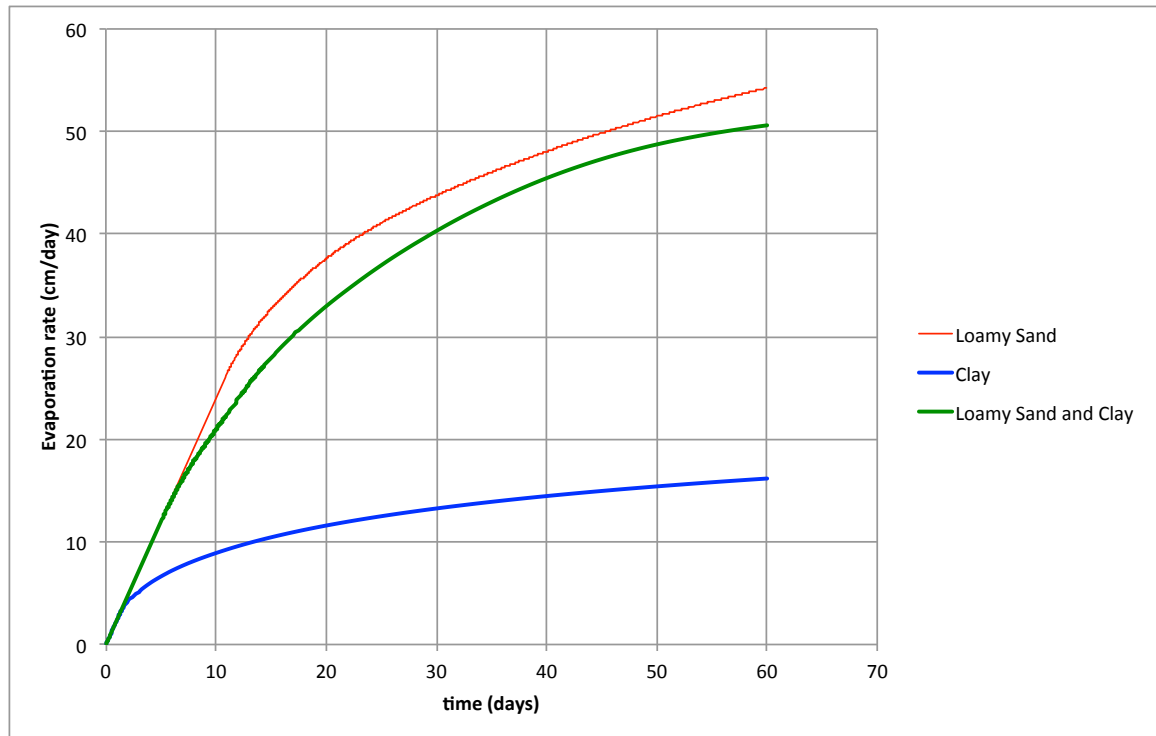
Figure 9: Results of HYDRUS simulation. Time evolution of the cumulative Evaporation of the non-synergizing bi-texture comprised of Loamy Sand & Clay and of its homogeneous counterparts.

The laboratory experiments that used Sandy Clay malfunctioned due to the proportion of clay that was used in generating the Sandy Clay texture. It was found that the laboratory Sandy Clay behaved more like a Clay. Therefore, we include here the HYDRUS simulation results for the bi-texture Loamy Sand & Clay (Figures 8 and 9) for use in later discussion of the results of the laboratory experiments..

Table 2. Discrepancies between the equations by Lehmann *et al.,* (2008) for the depth to the drying front (L_{S1}) at t_{S1} (Eq. 7) and the HYDRUS predictions, and the discrepancies between Nachshon's (*et al.,* 2011) equation for t_{S1}, the final system t_{Step}, (Eq 8) and the HYDRUS predictions.

	t_{S1} Depth (cm)		t_{S1} (days)	
	no viscous dissipation	with Lv Prediction	no viscous dissipation	with Lv Prediction
Texture	(Eq 8)		(Eq 9)	
Sand	2.3	7	5.7	8.2
Clay	290.1	<1	185.6	0.9
Silt Loam	46.5	3	30.6	9.5
LS & L	-	4	24.7	6.2
L & SiCL	-	1	96	5.6
CL & SiC	-	<1	20	<1

As stated in the theory section, equations 4-9 that predict values for the duration of stage 1 and the depth of the drying front at the end of stage 1 are all derived from linear head and saturation relationships that would not accurately represent a the wider pore size distribution of soil. Table 2 shows the differences between numerical values versus those predicted by equations 8 and 9 from previous studies. In addition to the issues related to the linearization of the moisture release curve, the equations do not account for viscous forces within finer soils that would interfere with the L_G and L_C relationships (ref. Eqs 4-8). It is suspected that for these reasons these two equations do not accurately predict characteristic lengths or t_{S1} for finer soils, and Table 2 shows how large the discrepancy is.

The depth of the drying front in the synergizing and non-synergizing bi-textures is shown as a function of time in Figures 10, 11, and 12. In the synergizing bi-texture (Fig. 10), the moisture content for the coarse and fine media are graphed with depth for 5 specific times corresponding to the 5 steps of stage S1. The values for Table 1 were taken from this figure. It is important to note that the fine media is extracting moisture from the coarse

at successively greater and greater depths. Similarly, the non-synergizing bi-textures (Figs. 11 and 12) show the moisture content for their respective steps of S1 evaporation. It is important to note, although not shown in the graphs, that within the synergizing combination the drying front of the coarse media moves downward at a rate that is far greater than it would under homogeneous conditions, while the fine textured media does not move. Figure 10 partly exemplifies this difference. The drying front behavior is very different for the non-synergy case. Figure 1 shows that the fine media (Sandy Clay) was unable to extract enough moisture from the coarse (Loamy Sand) before itself transitioning into S2 to cause much of a drop in the second drying front within the coarse (~2 cm).
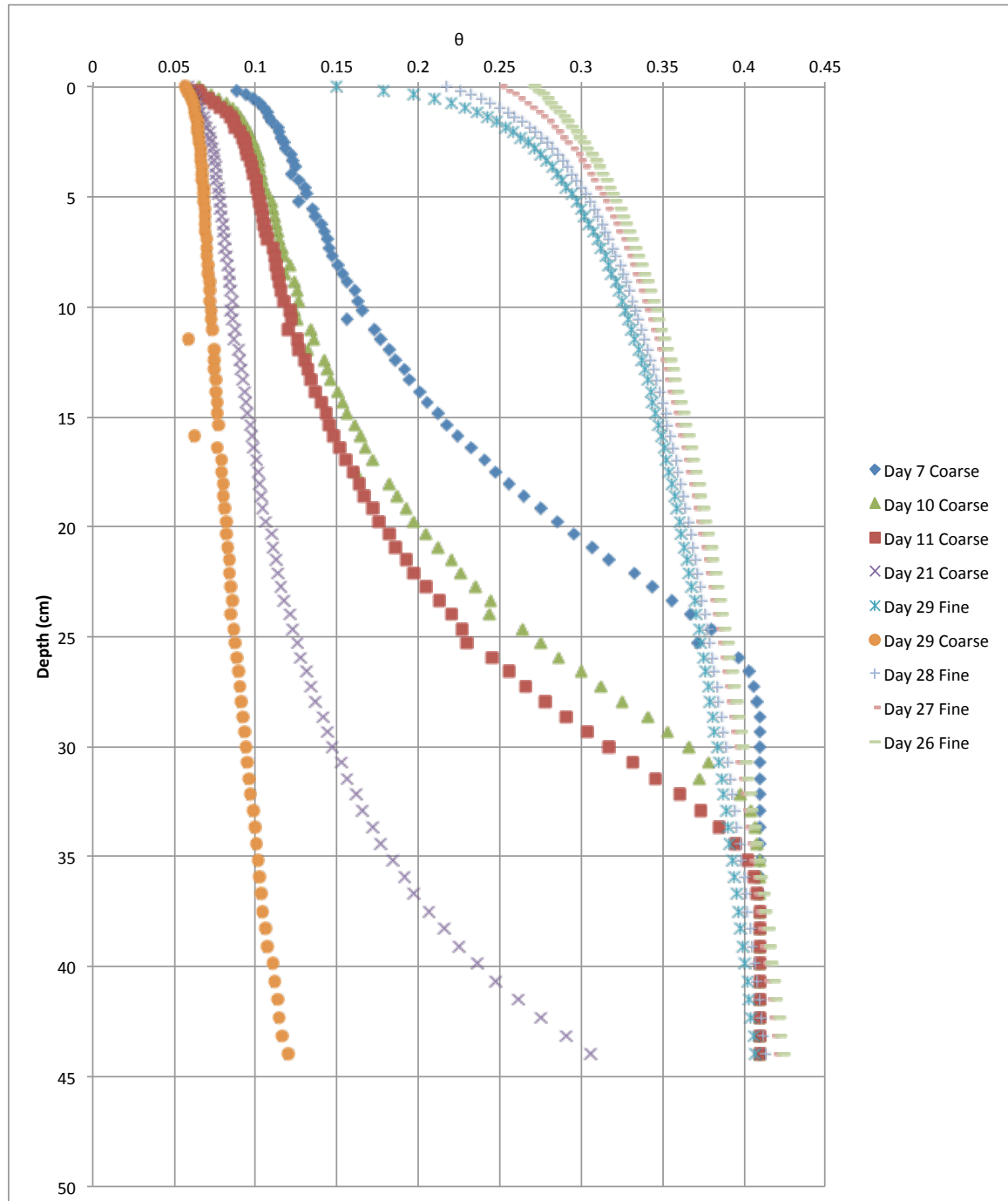
Figure 10. Volumetric moisture content (θ) as a function of depth for the synergistic bi-texture of a Loamy Sand & Silt Loam. The moisture profile is plotted separately for the coarse and fine portions. Days 7-11 represents each t_{S1} 'step' for the coarse until a final system crash into stage 2 evaporation at day 29 when the fine portion finally transitions into S2 stage.

During days 26-29 the fine texture shows the gradual loss of film connections to the evaporating surface until end of S1 at t_{S1} = 29 days.
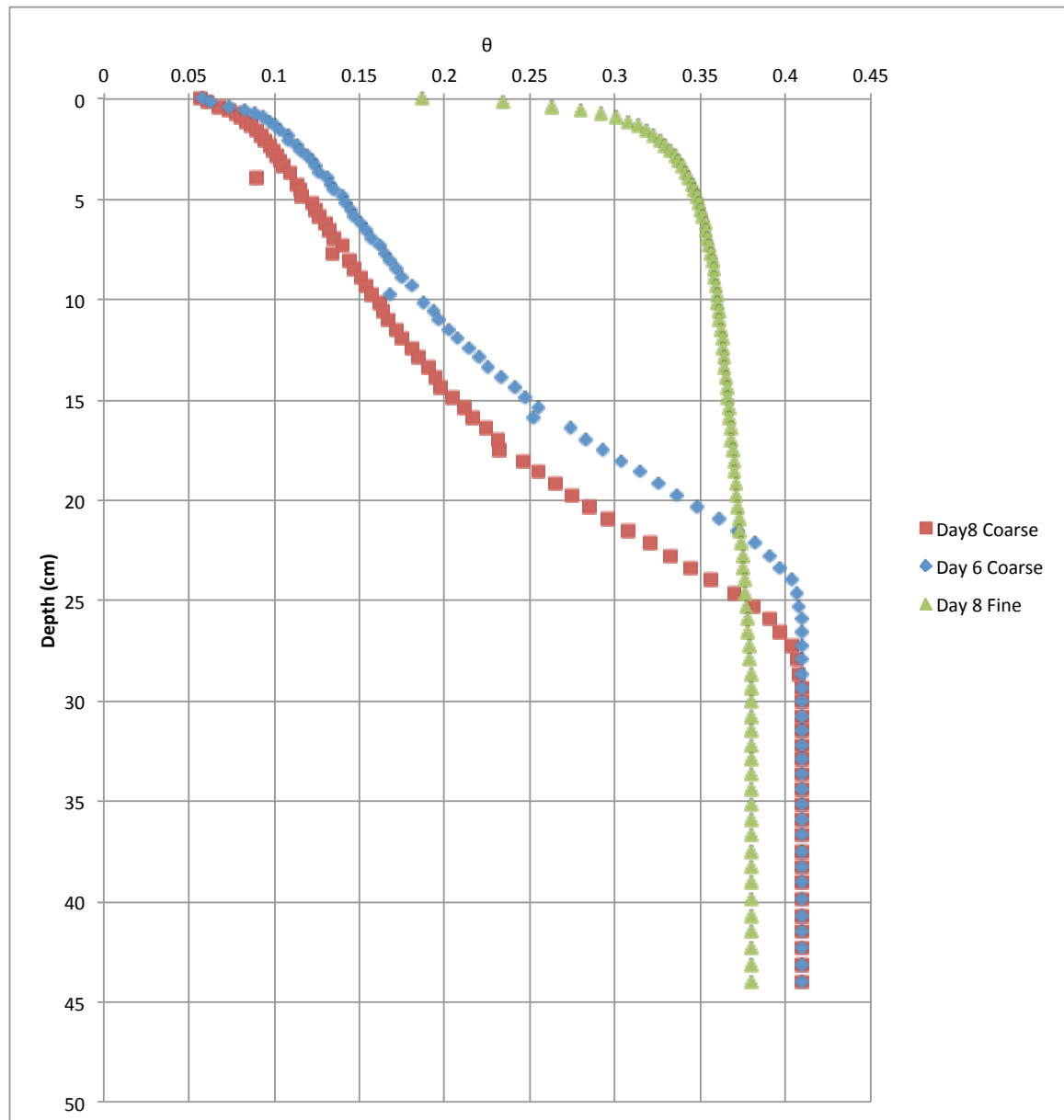
Figure 11. Volumetric moisture content (θ) as a function of depth for the non-synergistic bi-texture of a Loamy Sand & Sandy Clay. The θ is plotted separately for the coarse and fine portions. Day 6 represents the t_{S1} for the coarse until a final system crash into stage 2 evaporation at day 8 when the fine portion leaves S1 at t_{S1} = 8 days.

Figure 12 shows the progression of the drying front for the enhanced evaporation pair Loamy sand & Clay. It does not exhibit any characteristics that are exceptional to the synergistic pair shown in Figure 10, but is included here for completeness to assist in the discussion of the laboratory work.
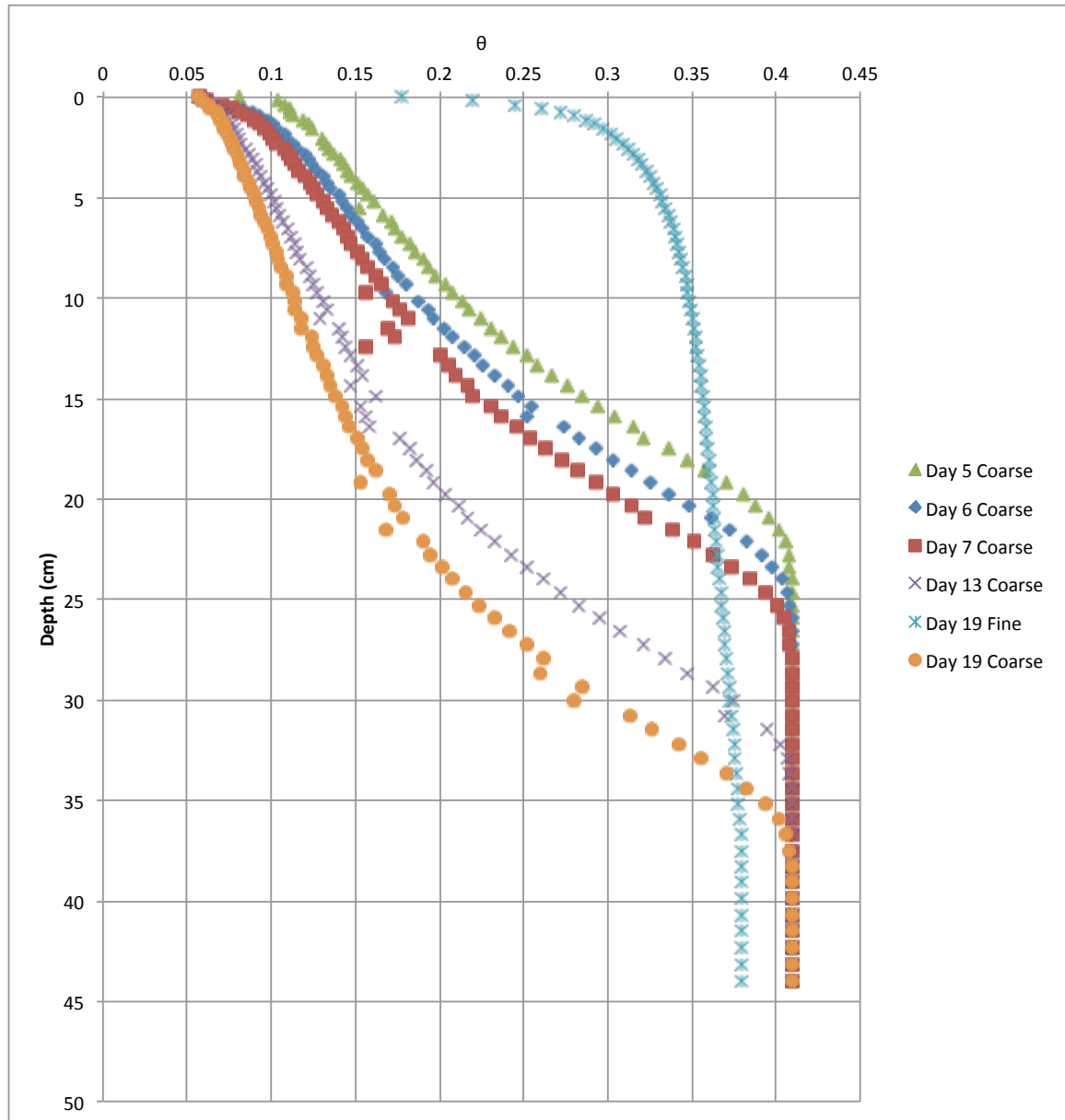
Figure 12. Water Content (θ) as a function of depth for the synergistic bi-texture of a Loamy Sand & Clay. The θ is plotted separately for the coarse and fine portions. Days 5-13 represent each t_{S1} for the coarse until a final system crash into stage 2 evaporation at day 19 when the fine portion leaves t_{S1}.

Figures 10, 11, and 12 illustrate the wetting front travelling

downward at different rates in the coarse and fine portions. The most

important piece of information from these graphs is the ability to see at what drying front depths of the coarse media the different t_{Steps} occur. Furthermore, the Loamy Sand & Silt Loam bi-texture exhibited such strong evaporation synergy characteristics that the system was able to nearly drain the entire coarse portion of all moisture. Between days 21 and 29 the coarse texture drying front intersected the bottom no-flux boundary. The model was re-run with a deeper column but serendipitously this did not affect the duration of the fine S1. In general, numerical models need to be large enough so that the column depth is greater than L_v+L_{cap}. In the non-synergy cases, the bi-texture still participated in lateral transfer of moisture. Although the finer portions remained more saturated in all cases than it would have under homogeneous conditions, the system was not able to deliver more moisture to the atmosphere than either homogeneous texture. This is discussed in greater detail in the Discussion section.

Graphical displays of the HYDRUS numerical results for the synergizing (Figure 13) and non-synergizing (Figure 14) pairs display the extreme difference in the evolution of the moisture content through time. The synergizing pair (Fig 13) shows the extreme lowering of the drying front of the coarse shown in (similar to Figure 10). The non-synergizing pair (Fig. 14) shows a much higher moisture content within the coarse compared to that within a synergizing combination. The graphs further emphasize the enhanced lowering of the drying front within the coarse in a synergistic texture combination.
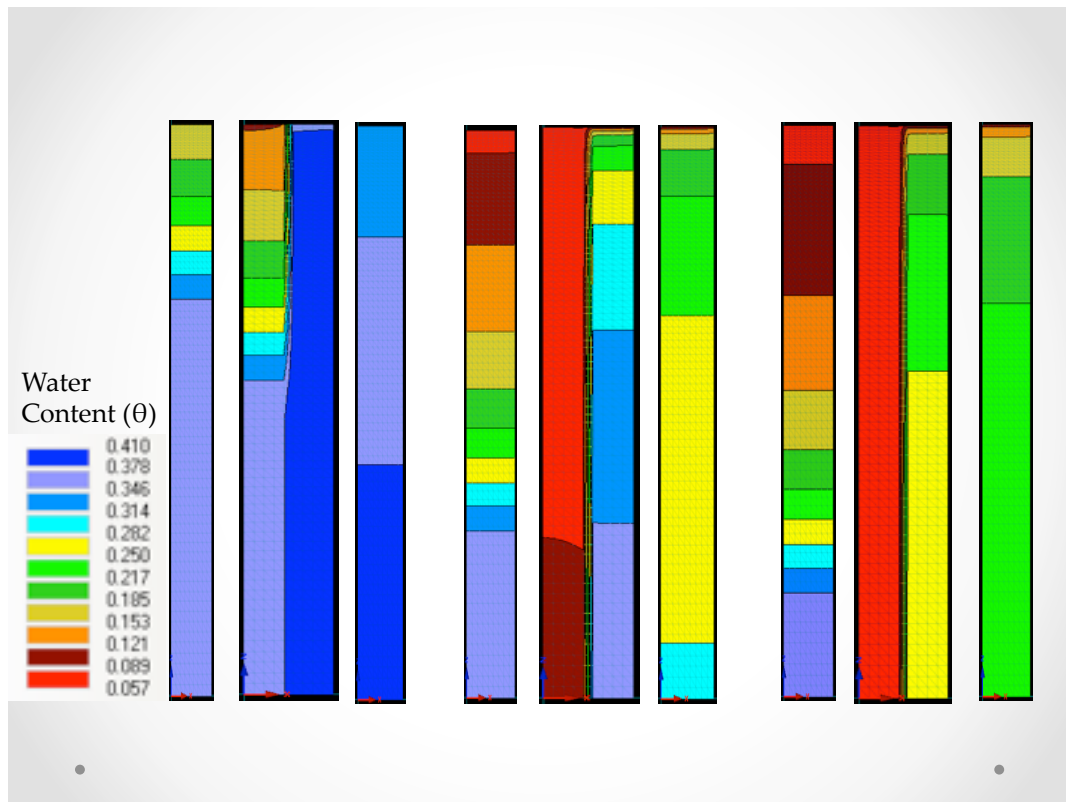
Figure 13. Results of HYDRUS simulation for moisture content profile. Loamy Sand (left-hand side) & Silt Loam (right-hand side) at 5, 30, and 60 days with homogeneous counterparts on either side. Results show the drying front of the coarse media moves downward at a rate that is far greater than it would under homogeneous conditions, while the fine textured media does not move until coarse is nearly drained.
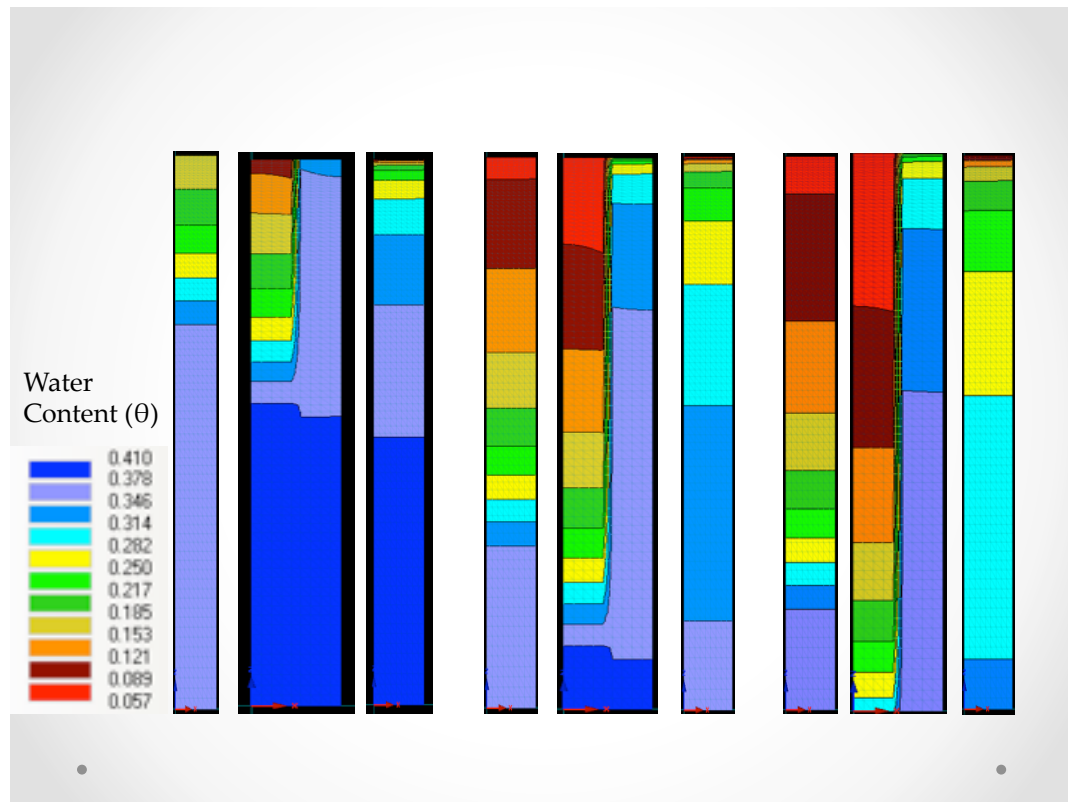
Figure 14. Results of HYDRUS simulation. Moisture content profile for Loamy Sand (left-hand side) & Sandy Clay (right-hand side) at 5, 30, and 60 days with homogeneous counterparts on either side.

Hydrus results were used to calculate the proportion of moisture that is lost to the atmosphere from each texture as the evaporation process progresses (Figures 15 and 16), for the synergy and non-synergy pairs. Notice how the fine texture in the synergy pair gradually loses more moisture as the coarse begins to dry out, or better said, as the drying front of the coarse goes deeper the fine texture has to exert more energy to pull water from the coarse portion to sustain stage 1 evaporation. In synergy, the Clay is initially losing ~20% of the system's moisture and is eventually responsible for losing ~40% of the moisture. Conversely, the non-synergy fine, the Sandy Clay, is initially responsible for losing ~10% of the moisture but by the end of the 100 day period only ends up losing ~20% of the

system's moisture. While it may appear from comparing Figures 15 and 16 that for the non-synergy case the coarse is able to lose a lot more moisture than under synergy, this is not true. These values do not represent net mass lost, but rather relative proportions. Note that the entire non-synergy system transitions into S2 relatively early. So, yes, the coarse does provide more water than the fine for a very long period of time, but it is at a very low diffusive rate. In all stages, it remains that the vast majority of the water loss is occurring from the coarse media.
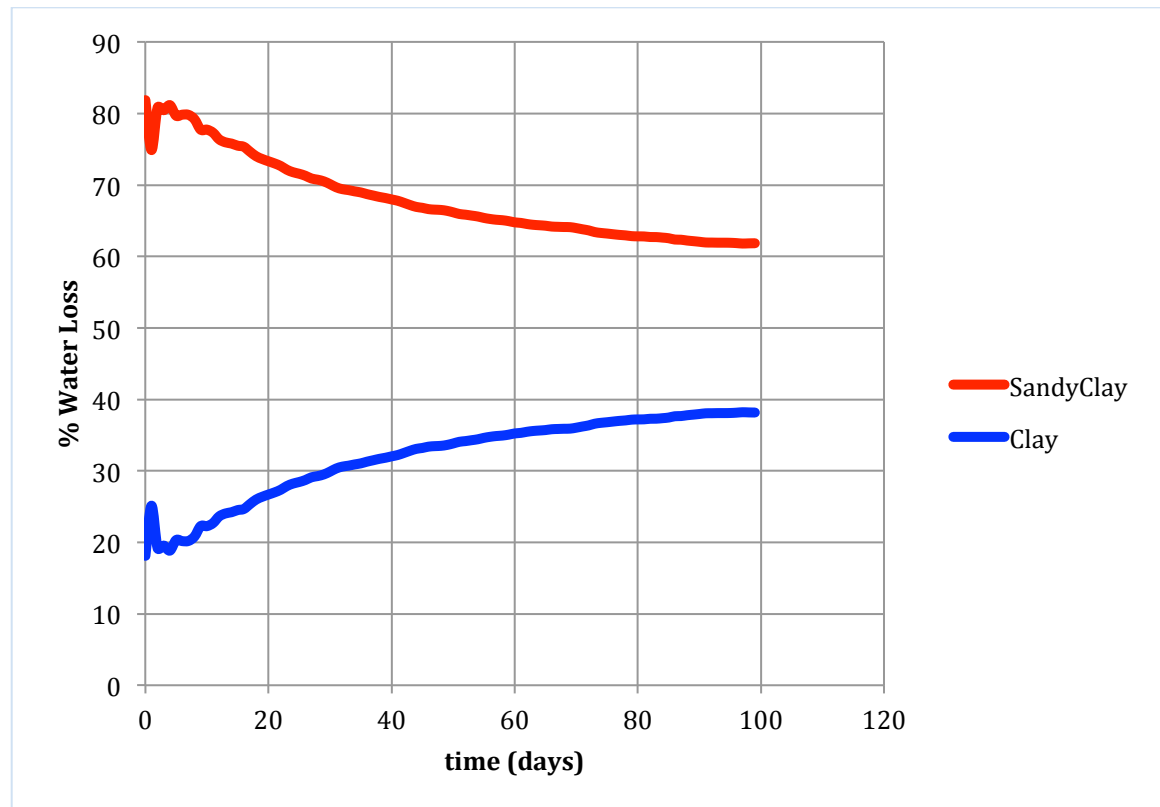
Figure 15. HYDRUS simulation results for the synergy pair Sandy Clay & Clay. Graph shows the proportion of water loss per unit time from each member of the bi-texture, calculated as % water loss from a texture relative to total water loss from the system. S2 transition for this bi-texture is at approximately 1.5 days.
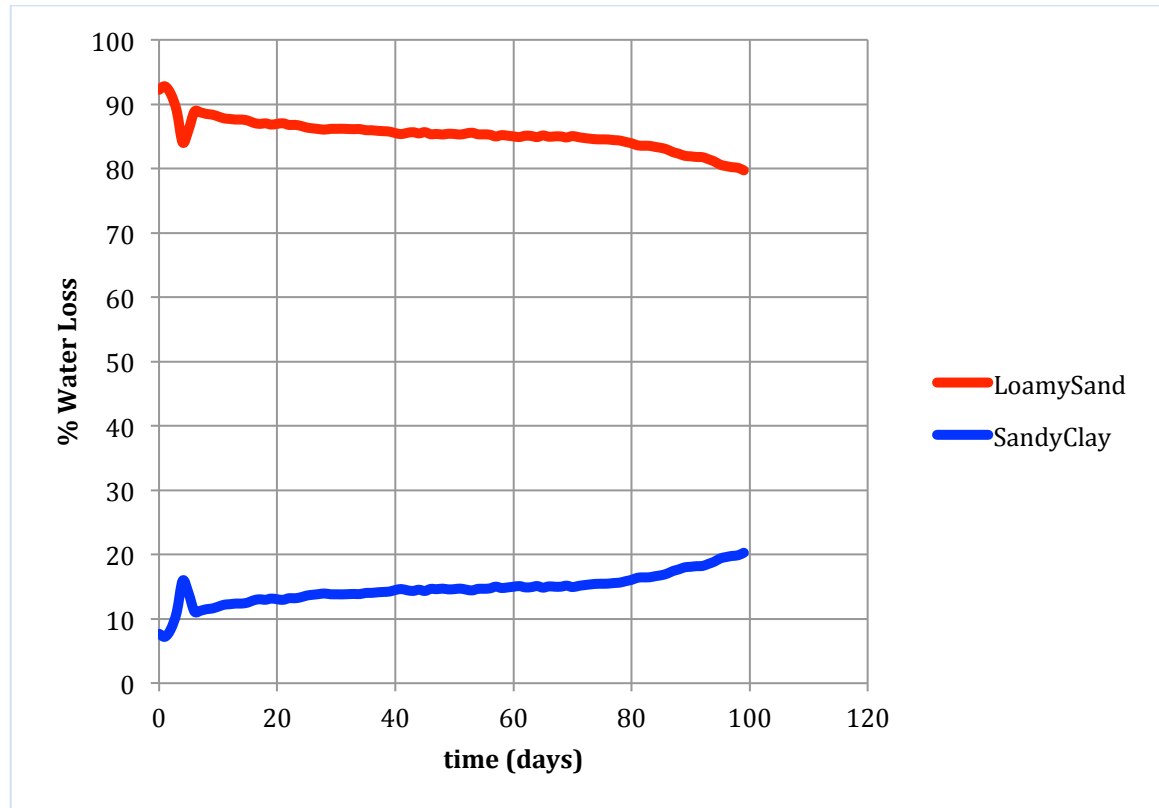
Figure 16. HYDRUS simulation results. Proportion of water loss per unit time from each member of the bi-texture, calculated as % water loss from a texture relative to total water loss from the system.

4.2   Results from Laboratory Experiments

Laboratory experiments using physical models similar in properties to the HYDRUS numerical models were selected especially to test if the synergistic phenomenon for soils was merely a numerical artifact or a real phenomenon. In addition it permitted showcasing of several interesting aspects of evaporation synergy. Two different combinations of soils were chosen to represent a bi-texture that would exhibit evaporation synergy, Loamy Sand & Silt Loam, and one that would not, Loamy Sand & Sandy Clay. It was decided to have the same coarse soil texture in common to both of the physical models, the Loamy Sand, to demonstrate the varying

effects of the same coarse media. Each bi-texture soil column was placed in an evaporating chamber with a controlled and constant evaporation rate of approximately 0.4 cm/day. Each experiment run consisted of 4 columns in the chamber, one with the bi-texture, two each with a homogeneous counterpart, and a DI water filled column (aka., water blank) to track the potential evaporation rate, details are described in the Materials and Methods. Having all the columns in the chamber at the same time was necessary for comparisons between columns under nearly identical climatic conditions.

Figures 17 and 18 show the raw data for the mass lost from the soil-water column and the cumulative evaporative losses from the synergizing Loamy Sand & Silt Loam pair, respectively. The combination which did not exhibit evaporation synergy is shown in Figures 19 and 20 where mass lost and cumulative evaporative losses, respectively, contrast the results of the synergizing pair. These combinations were chosen using the HYDRUS predictions and their relative evaporation behaviors agreed with the numerical results. The Loamy Sand & Silt Loam (Fig 18) did indeed lose more water to evaporation than either homogeneous counterpart, and the Loamy Sand & Sandy Clay (Fig 20), albeit exhibiting some level of enhanced evaporation (discussed later), experienced losses that were in between that of the homogeneous textures.
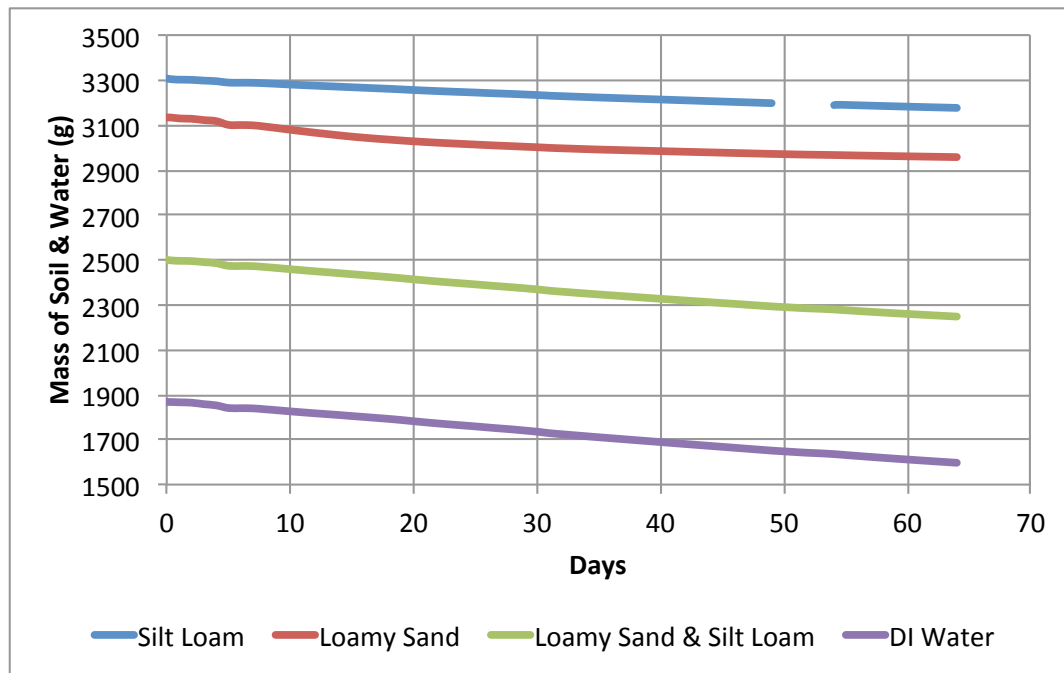
Figure 17. Raw data of mass loss for the four columns in the synergy experiment.
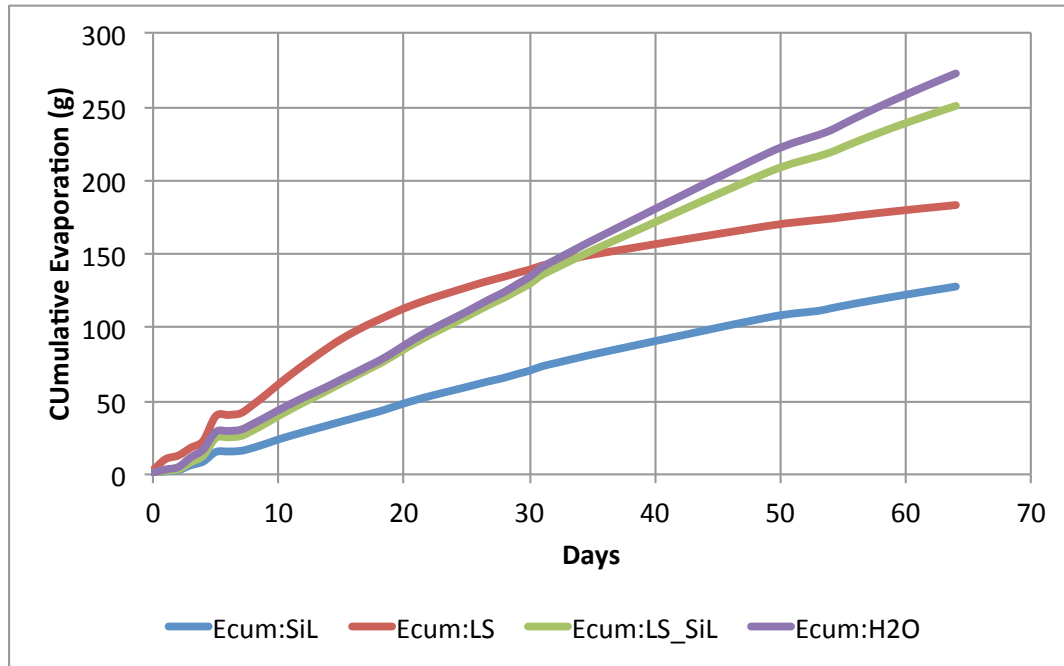
Figure 18. Cumulative evaporative losses for the four columns in the synergy experiment. The trend line for the water blank data shows a nearly straight line with a slope of 3.7 with a slight deviation after 45 days.

Note that the laboratory data is in grams of water while the HYDRUS data is reported in cm of water. In this case the units are interchangeable once the laboratory data is divided by the cross-sectional area of the column (10 cm^2). This is because in Hydrus an evaporation loss of 1 cm refers to a 1 cm height of water per 1 square centimeter of cross-sectional area. This gives a volume of 1 cubic centimeter, which for water and only for water, is equivalent to 1 gram of water (density of water being 1 g/cm^3).

The bi-texture combination of a Loamy Sand & Silt Loam exhibited evaporation synergy, as illustrated by the green line being higher than the red and blue lines in Fig 18. Note that it follows very closely to the potential evaporation rate line (purple). The water blank marks the maximum amount of evaporative demand within the chamber with two exceptions due

to technical problems in this particular experiment. During the first ~30 days the Loamy Sand lost much more water than the water blank: this water loss was caused by a leak between the lower sections of PVC. A second problem during this experiment is that the level of water was allowed to drop in the water blank by about 10 cm. The 10 cm of air head above the water may have slightly reduced the evaporation rate by increasing the relative humidity in that semi-confined upper 10 cm of column space: this may be seen by a slight decrease in the potential evaporation rate during the later stages of the experiment. It should be noted that moisture movement in the entire chamber was by diffusion and not by fan driven advection. Both of these problems will be further analyzed in the discussion section. The water loss due to evaporation at the end of 63 days is shown in Table 3. The bi-texture lost 27% more water than the Loamy Sand and 51% more water than the Silt Loam.

The bi-texture combination of a Loamy Sand & Sandy Clay did not exhibit evaporation synergy as illustrated by the green line failing to remain higher than the blue and red lines in Figure 20. Note that the Sandy Clay over takes the bi-texture after approximately 29 days. This indicates that an earlier transition to S2 was reached much earlier for the Sandy Clay in the bi-texture than in the homogeneous condition. The bi-texture lost 3.2 % less water than the homogeneous Sandy Clay and polynomial trend lines show evidence of a continuing divergence between the two.

Table 3. Water loss due to evaporation at the end of 60 days for each column in the synergy and the non-synergy experiments.

Synergy Experiment		Non-Synergy Experiment	
Water blank	276.48 g	Water blank	134.91 g
Loamy sand	184.7 g	Loamy sand	110.67 g
Silt Loam	129.22 g	Sandy Clay	128.53 g
Bi-texture	253.64 g	Bi-texture	124.39 g
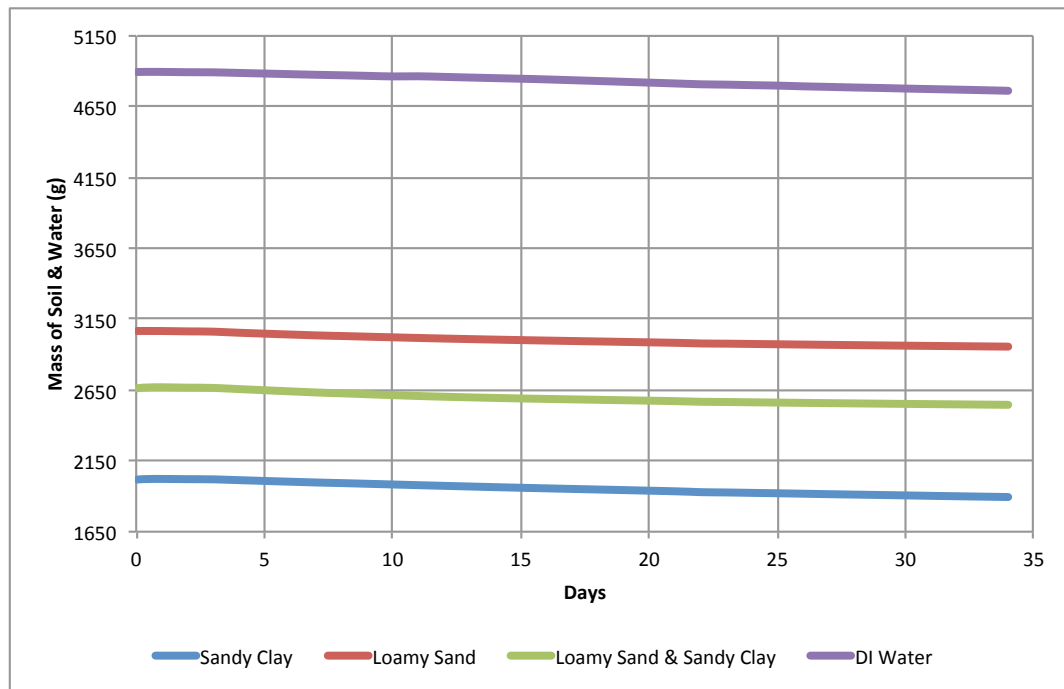
Figure 19. Cumulative evaporative losses from the four columns in the Non-Synergy experiment.
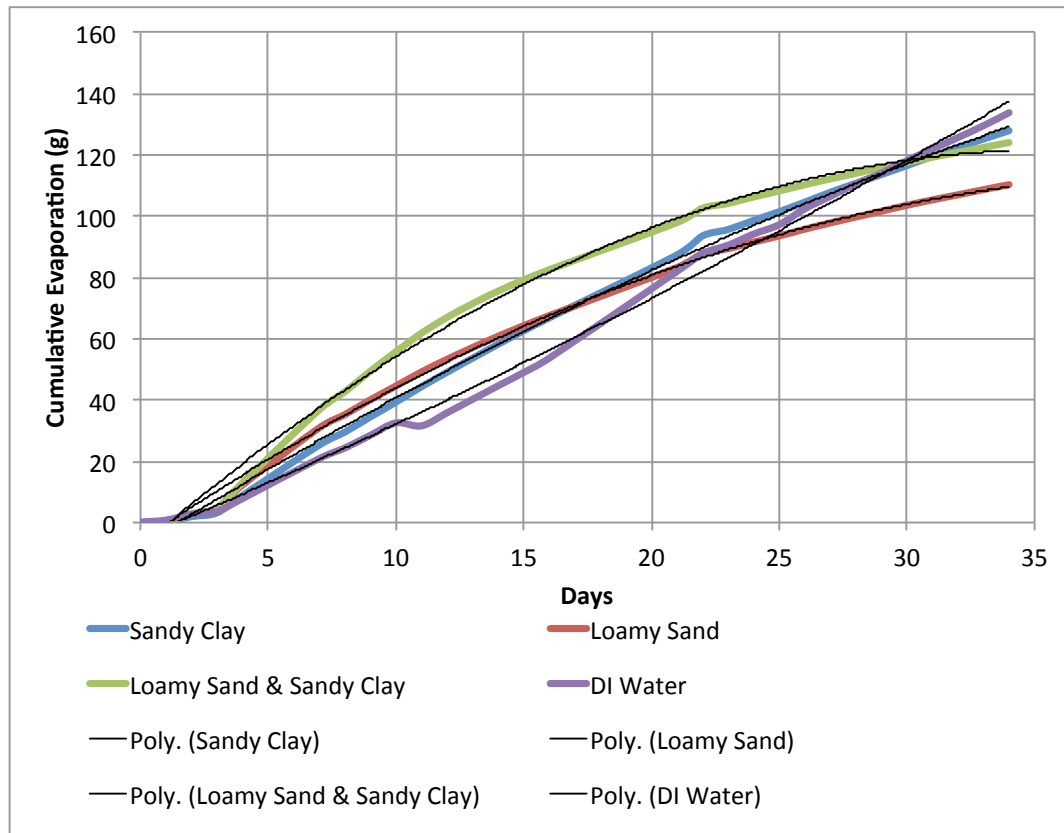
Figure 20: Cumulative Evaporative losses from the Non-Synergy experiment.

The large degree of scatter in the evaporation rate graphs (Figure 21) makes it difficult to distinguish the various steps of stage 1, or even the net duration. However, the cumulative evaporation curves unambiguously show that one bi-texture synergized and the other did not, as predicted by the numerical models. Furthermore, comparison of the slopes of the cumulative evaporation graph provides some indication of these differences (Fig 18). In the case of synergy, considering the mass of water lost over the last 12 days of the experiment the homogeneous Silt Loam and Loamy Sand had slopes of 1.4 g/day and 0.83 g/day, respectively. The water blank and heterogeneous Loamy Sand & Silt Loam had slopes of 3.7 g/day and 2.9 g/day, respectively. This is suggestive of a lengthened t_{S1}

duration within the bi-texture as its final 12 days of evaporation loss slope was much higher than either homogeneous texture and very close to the potential evaporation rate of the chamber.
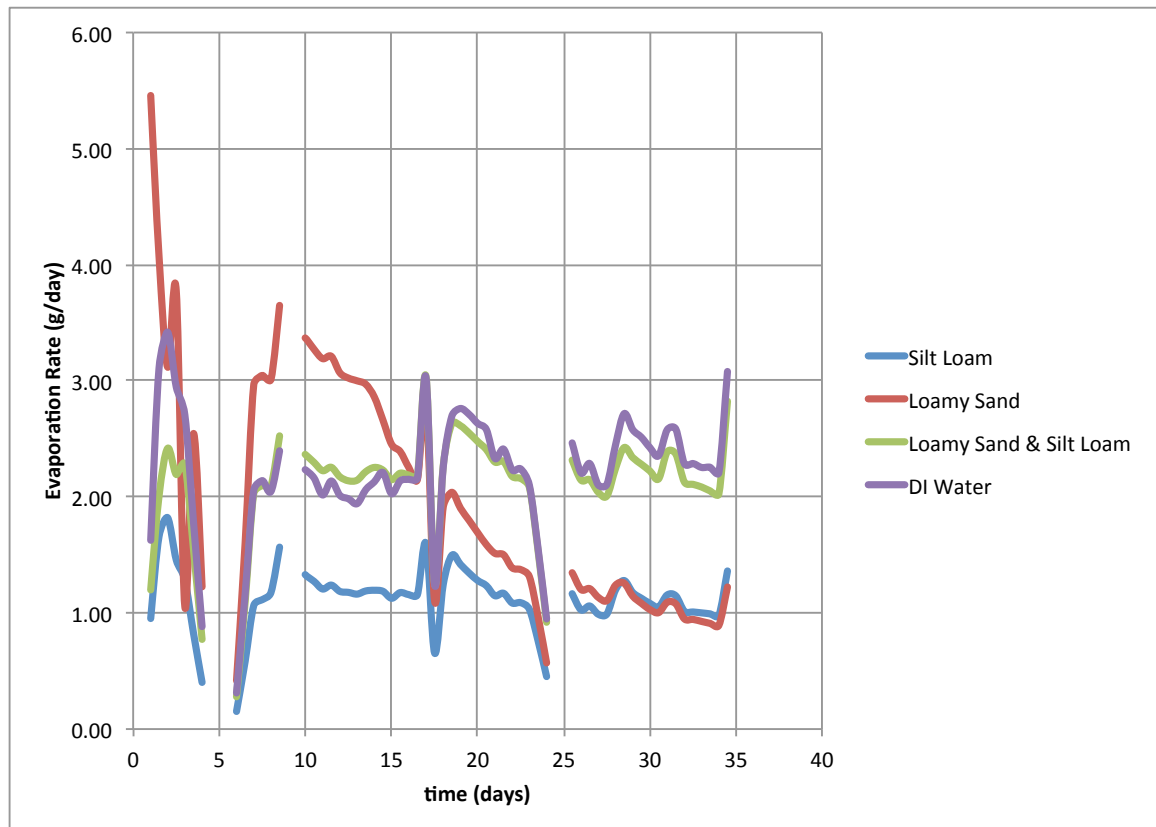
Figure 21. Evaporation rate (grams of water lost/day for the entire column) for the synergy laboratory experiment. Data calculated by taking 0.25 hour averages of 10 minute data.

5.   Discussion

At first glance, evaporation Synergy might appear to be the result of numerical model errors or failure to perceive design flaws in physical models. However, numerous studies have utilized both methods and have results similar to those in this paper. Studies by Nachshon et al., (2011 a and b) involved similar set ups with coarse and fine media but incorporated salt accumulation and found increased and preferential evaporation from the fine media. Or (et al., 2007) conducted this type of experiment and also found an earlier drying front propagating in the coarse media while the fine remained saturated. Lehmann and Or's (2009) study most resembles the methods in this paper and mentions enhanced evaporation in a bi-textured system. Their results were corroborated by the Shahraeeni and Or's (2010 and 2011) studies. These follow up experiments utilized Infrared Thermography to confirm Lehmann and Or's (2009) results as well as the lateral transfer of water within a heterogeneous porous media after the coarse had reached air entry value expressed by:

$$\Delta h_{cap}=h_b{}^f-h_b{}^c \qquad\qquad \text{Eq. 11}$$

where a difference in driving capillary force is created by the difference between the air-entry values of the coarse and fine. The driving capillary force supplying water flux to the surface (at a rate of Q_E) must be matched by the coarser texture's ability to laterally supply water (at a rate of Q_H) to the fine. If this condition is not met the fine texture will become hydraulically disconnected from the evaporating surface and transition into the slower vapor-diffusion controlled stage 2 evaporation. The texture's ability to laterally supply water to the fine and the fine's ability to carry water to the surface highlight the main difference between previous studies and this study. All of these previous studies support the legitimacy of evaporation

synergy but in a fine and coarse *sand* system instead of a fine and coarse *soil* system. Although the vertical and lateral pressure differences will form in any coarse/fine combination it is the limiting viscous forces, conductivities, and capillarity forces within soils - that are not found in the relatively coarse sands but may be found in finer textured soils - that may inhibit evaporation synergy in soil systems. Therefore, the same principal mechanisms apply to both sand and soil systems but evaporation synergy is dependent on a slightly more complex combination of porous media properties within a soil system than may have been evidenced by the sand studies. The role of viscous dissipation was mentioned by Lehmann (*et* al., 2008), but has not been incorporated into any of the models prior to this work and is the reason why previous studies do not explain soil behavior. The equations that deal with air-entry values and evaporation sustaining flow (Eq.'s 2 and 3) are basic conditions necessary for synergy to take place. They represent the pressure gradients crucial for sustaining flow throughout the system. Similarly, this is also why the "$t_{S1}{}^{c}$<$t_{S1}{}^{f}$" relationship is legitimate as it is a general rule for bi-textures to sustain a reservoir/wick relationship between the coarse/fine textures. However, the other equations involving Lehmann's (*et al.*, 2008) characteristic length equations (Eq.'s 4-8) do not apply to soils which are much finer and have a broader particle size distribution than well sorted sands. This, in extension, is why Nachshon's (et al., 2011(a)) t_{S1} prediction (Eq. 9) is not accurate for finer soil textures. All variables rely on a characteristic length that largely ignores the viscous forces within the finer soils – which are non-negligible for soil - making it unreliable when predicting specific limiting drying fronts for soils and specific times for evaporation stages. Thus, these equations do not accurately predict characteristic lengths or t_{S1} for finer soils and deriving new equations for soil is necessary. While the work presented

here establishes the need for new, more complete equations, it is beyond the scope of this work to derive these equations.

Lehmann and Or's (2009) study included numerical simulations in which the Carsel and Parrish (1988) hydraulic parameters were used in conjunction with soils' conductivities, air-entry values, and potential evaporation rates. They were able to numerically determine a bi-texture's maximum radial distance (R_{max}) that directly relates to lateral flux (Q_H) and also depends on evaporative flux (Q_E). Their numerical predictions of soil combinations show a Loam/Sand combination extracting the largest amount of water through evaporation and have correspondingly large R_{max} values for the pair. While this study focused on columns of limited extent (10 cm diameter), to keep it relevant to laboratory work, a series of simulations was performed to investigate the role of scale on net evaporative loss. The series quantified cumulative losses from three scales of synergistic soil columns (Loamy Sand & Silt): a single width of the fine Silt (5 cm) was abutted against 3 different widths of the coarser Loamy Sand (5 cm, 15 cm, and 25, cm). Relative to the 5 cm + 5 cm column (mass loss of 127 cm at 100 days) the 5+15 cm and the 5+25 cm resulted in a 52% and 76% increase respectively. The wider column width made it possible for more water to be pulled laterally from the coarse and lengthened the duration of each S1 step. This increased the amount of evaporative synergy, as the fine was able to pull more water laterally. This is due to the lateral viscous forces (L_V) being less at a higher depth than the difference in the vertical gravitational forces (L_G) at a lower depth. Simply put, the fine will pull water laterally, where there are no gravitational forces to overcome, as long as the viscous forces are smaller than the gravitational and viscous forces at a lower depth (Appendix 2).

As mentioned earlier, S1 stage for a bi-texture is not constant but comprised of a series of decreasing steps in constant evaporation (e.g., Fig. 4). The occurrence of these steps is an oddity seen in the evaporation rates of all bi-textures from the numerical models and also in one published laboratory evaporation experiment (Nachshon, et al., 2011). The previous published studies, mentioned earlier in this section, determined that there is a reservoir/wick relationship between the coarse/fine textures during evaporation. It is proposed here that the following scenario causes the existence of the steps. The tension in the coarse increases as the fine draws water from the front. As the water content in the coarse portion becomes too low the K(h) becomes too slow increasing the viscous dissipation value reducing the ability of the fine texture to pull water toward itself. Once this happens, the drying front within the coarse portion drops to a new level where K(h) is greater and viscous dissipation less, permitting the fine media to extract water from this depth. The result of this drop in the level from which the fine extracts water causes a decrease in evaporation rate. And, the evaporation rate will stay at that level until the fine has extracted all the water it can laterally from that depth. In essence, every t_{Steps} represents the duration of time that the coarse reservoir can laterally supply water to meet the fine wick's Q_E at a certain depth until the tension becomes too high for the coarse to maintain lateral flux (Q_H). Once the situation is reached where the fine wick can no longer pull water from deeper portions of the coarse without exceeding its own critical value (h_f), the fine texture enters stage 2 evaporation.

Figure 22 illustrates the process just described with generic matric potential (ψ) v. water content (θ) graphs for a synergizing bi-texture. When both textures are in S1 evaporation they are under saturated conditions and it requires relatively little tension/suction for the atmosphere to remove

water from their evaporating surfaces (S1a). At the First Step the coarse has reached the critical value, initiating S2 and it is at this point when the fine starts to laterally pull water from the saturated portion of the coarse that is hydraulically disconnected from the evaporating surface. At S1b the fine continues to pull water laterally from the coarse until the coarse reaches a second drying front depth. There are two things to keep in mind during this transition: 1) the fine has managed to satisfy it's own evaporative flux by exerting suction on the water within the coarse and 2) the suction within the fine is not sufficient to overcome the diminishing $K(\theta)$ within the coarse to supply water at this depth. Consequently, the fine starts to pull water from a lower depth in the coarse (S1c) until a 3rd Step is reached at an even higher tension. At this point the fine can no longer exert the necessary suction on the water at such a low depth within the coarse. Following this, the fine will lose hydraulic connectivity to its evaporating surface and the entire bi-texture system will crash into S2 evaporation.
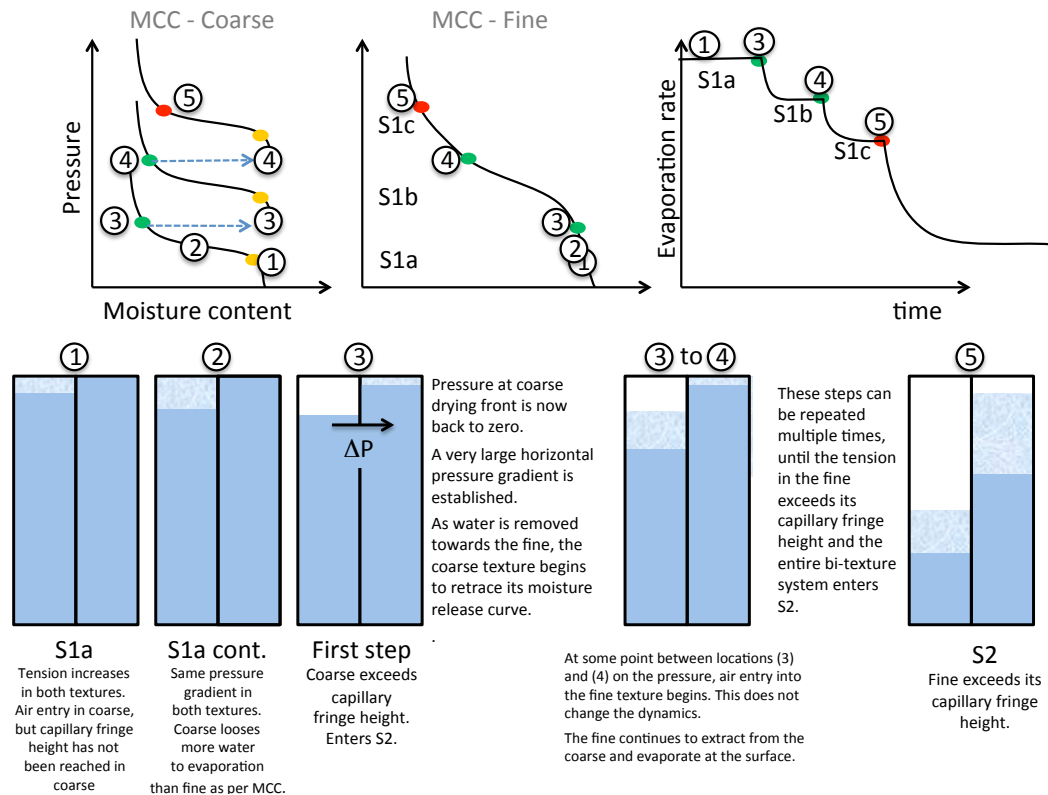
Figure 22. Illustration of the step process of a synergizing bi-texture. The coarse and fine textures are on the left and right, respectively, of each column. The drying of the system progresses from left to right in the bottom series of figures. The numbers atop each columns sketch refer to the moisture condition on the moisture release curves on the upper half of the figure.

The following two paragraphs discuss some difficulties in the experimental work, and whether these difficulties impact the conclusions of this work.

The non-synergy laboratory results were not as straightforward as planned. The intent of the non-synergy laboratory column was to compare it to the Loamy sand & Sandy clay numerical model results. However there was a problem in the process for obtaining a Sandy Clay that caused the results to differ. It was decided to create a Sandy Clay by combining fine sand with kaolinite in a 50/50 mixture. The high percentage of clay in the

mixture expressed too much of a clay's characteristics and the sand particle size did not affect evaporative or hydraulic functions within the Sandy Clay portions. Therefore, the Sandy Clay behaved more like a Clay. And the corresponding bi-texture was more representative of a Loamy Sand & Clay. The trend lines for cumulative evaporation data for the laboratory column shows the bi-texture initially exceeding the homogeneous 'Sandy Clay' but eventually being overtaken by it and continuing to diverge (Figure 9). This mirrors the HYDRUS model for a Loamy Sand & Clay where the bi-texture has a higher E_{rate} and E_{cum} for a period of time but cannot maintain S1 long enough to show a higher cumulative evaporation amount than both of the homogeneous textures. Thus, the corroboration of the laboratory LS&SC with the numerical LS&C confirms that in our laboratory column our SC mixture behaved like a Clay. Even with this unexpected turn of events, the laboratory results mirrors the numerical results in the case of non-synergy.

Another experimental difficulty was a leak that developed in the Loamy Sand of the synergizing case. The leak was evident visually as well as by the fact that from day 5 – 18 the coarse lost more water than the water-blank. The leak seems to have occurred in one of the lower column junctions. This column was constructed of three PVC segments taped together with electrical tape. The leak is expected to have had the effect of lowering the evaporation rate by lowering the matric potential of the media (similar to downward drainage). This could have shortened the transition into S2 for the homogeneous column; however, the leak seems to have begun on day 5, well after the predicted transition to S2 on day 2 (predicted by the numerical model). And since the bi-texture continued along S1 at this time, the existence of the leak does not contradict the observation that the bi-texture did indeed lose more water than either homogeneous texture.

Furthermore, this leak would suppress synergy, not enhance it, so a positive result would remain positive even with this potential source of error.

The third problem was that the water level in the water-blank for the synergy case was allowed to decrease (to a maximum of 10 .3 cm by the end of the experiment). The decrease in evaporation rate due to a lowering evaporation front is seen by a slight bend in the curve in the potential evaporation rate for the chamber at late time. Ideally, a system would have been set up similar to that used in the non-synergy run where a hanging Marionette bottle would have kept the water surface near the surface of the column. For these reasons, the leaking Loamy Sand and water blank, the synergy experiment may have yielded less accurate results. But even with these two problems, the results still stand that the bi-textured exhibited significant synergy.

6.   Conclusion

This manuscript presents results from an investigation of evaporation from heterogeneous porous media, specifically the case where the heterogeneity interface intersects (normal to) the evaporation surface. The mechanisms were investigated numerically, with some support from new and published experiments. The goals of this study were to prove the existence of evaporation synergy in finer textured soils while determining the necessary conditions and part of the criteria for the phenomenon. An additional goal includes the identification of the particular soil texture combinations that resulted in evaporation synergy, the phenomenon in which two textures that share a vertical boundary experience higher cumulative losses to evaporation than either homogeneous texture can produce.

The numerical modeling software package HYDRUS was used to quantify the evolution of evaporation rates, cumulative evaporation amounts and evaporation dynamics for bi-textures comprised of all 66 combinations of soil textures. Following the numerical study, two representative bi-texture sets were chosen for laboratory testing to reflect the conditions of the numerical model in which the evaporation phenomenon is seen. This was necessary to have real world evidence for which to justify the numerical model's predictions of Evaporation Synergy and Non-synergy in a bi-textured soil system.

One might assume that the mechanisms that drive evaporation from heterogeneous media would result in simply averaging the amounts of water lost from individual textures. This might be true if not for the mechanisms that act across the boundary of vertically paired porous media with different textures. Both published and new laboratory experiments presented here have shown evidence of evaporation synergy. The

numerical simulations permitted expanding these tests over a wider range of porous media properties than practical by laboratory methods. The simulations also made it possible to observe evaporation rates and cumulative losses in a perfectly packed and saturated soil media as well as the depths for each drying front during evaporation. This information was essential to understanding how lateral viscous forces as well as vertical gravitational forces affect evaporative ability within a porous medium. Simulations also made it possible to observe the effect from texture combinations of different dimensions. It was found that a wider coarse reservoir leads to higher cumulative losses from the system. This is due to the relative extra lateral reservoir from which the fine can pull water while competing against only viscous (and not gravitational) forces.

The numerical simulations predicted 20 out of the 60 texture combinations resulted in evaporation synergy with evaporative losses in between ~5% to ~20% greater than either homogeneous texture. In the laboratory, the cumulative evaporation from a Loamy Sand & Silt Loam bi-texture lost at least 27% more water over 60 days than either of its homogeneous counterparts. All of the laboratory work previously published was limited to using well-sorted sands as the porous media. This was the first investigation where soil was used. The correlation between the laboratory experiment and the much more extensive numerical work validates evaporation synergy as a real world soil-water phenomenon.

Another consideration brought up by the numerical simulations is that the existing equations representing synergy criteria and those predicting evaporation properties do not apply to soils. Previous researches developed the equations from studying evaporation from well sorted fine and coarse sands, which do not account for very large viscous forces and broad particle size distributions. These viscous forces play a

major role in finer textured soils and greatly affect the porous-medium's ability to transport moisture. Thus, it has been shown clearly here that new equations are needed. While development of these new equations was beyond the scope of this work, the precedent that they are needed has been established.

This study made observations of the morphology of the evaporation rate curve as well as solidified the conceptual model for the synergistic process of a bi-textured soil. The morphology of the evaporation rate curve for a bi-texture takes on an additional feature: the first stage of evaporation decreases in a series of constant-rate steps until the fine transitions into S2 evaporation, marking the end of the system's S1. It is proposed that these steps are associated with a stepwise recession of the drying front in the coarse media. The duration of each step appears to be associated with the lateral distance from which water can be extracted within the coarse media. The criteria for synergy for the two textures include: different air-entry values to create the capillary barrier at the drying surface of the coarse texture thus establishing a reservoir/wick relationship between the coarse and fine, respectively; the fine must possess a high enough hydraulic conductivity and capillarity to allow water to move to its surface before it reaches its own critical value where liquid film flow is severed at the soils surface; and finally, the viscous forces within the coarse must be low enough for water to be pulled from itself to the fine. These are the conditions necessary for evaporation synergy to occur.

Bibliography

Abbasi, F., J. Feyen, M.Th. van Genuchten. 2003. Two-dimensional simulation of water flow and solute transport below furrows: model calibration and validation. Journal of Hydrology 290: 63–79.

Bechtold, M., S. H. Pohlmeier, J. Vanderborght, A. Pohlmeier, T. P. A. Ferré, and H. Vereecken. 2011. Geophysical Research Letters. 38: L17404, doi:10.1029/2011GL048147.

Carminati (b), A., A. Kaestner, H. Flühler, P. Lehmann, D. Or, E. Lehmann, and M. Stampanoni. 2007. Hydraulic contacts controlling water flow across porous grains. PHYSICAL REVIEW E 76, 026311.

Carsel, R. F., R. S. Parrish. 1988. Developing joint probability distributions of soil water retention characteristics. Water Resources Research. 24: 755-769.

Hillel, D. 1998. Environmental Soil Physics, p. 507-543 Evaporation from bare soil and wind erosion. Academic Press, San Diego.

Kandelous, M. M., J. Simunek, M. Th. van Genchten, K. Malek. 2011. Soil Water Content Distributions between Two Emitters of a Subsurface Drip Irrigation System. Soil Science Society of America Journal. 75: 488-497.

Kozak, J.A., and L. R. Ahuja. 2005(a). Scaling of Infiltration and Redistribution of Water across Soil Textural Classes. Soil Sci. Soc. Am. J. 69:816–827.

Kozak, J. A., L. R. Ahuja, L. Ma, and T. R. Green. 2005(b). Scaling and Estimation of Evaporation and Transpiration of Water across Soil Textures. Vadose Zone Journal 4:418–427.

Lehmann, P., and D. Or. 2009. Evaporation and capillary coupling across vertical textural contrasts in porous media. Physical Review E. 80, 046318, doi: 10.1103/PhysRevE.80.046318.

Lehmann, P., S. Assouline, and D. Or. 2008. Characteristic lengths affecting evaporative drying of porous media. Physical Review E. 77, 056309, doi: 10.1103/PhysRevE.77.056309.

Lehmann, P., P. Wyss, A. Flisch, E. Lehmann, P. Vontobel, M. Krafczyk, A. Kaestner, F. Beckmann, A. Gygi, and H. Flu˙hler. 2006. Tomographical Imaging and Mathematical Description of Porous Media Used for the Prediction of Fluid Distribution. Vadose Zone Journal 5:80–97.

Metzger, T., and E. Tsotsas. 2005. Influence of pore size distribution on drying kinetic: A simple capillary model. Drying Tech. 23: 1797-1809.

Nachshon. U., E. Shahraeeni, D. Or, Maria Dragila, and N. Weisbrod. 2011(b). Infrared thermography of evaporative fluxes and dynamics of salt deposition on heterogeneous porous surfaces. Water Resources Research. 47: W12519, doi:10.1029/2011WR010776.

Nachshon. U., N. Weisbrod, M. I. Dragila, and A. Grader. 2011(a). Combined evaporation and salt precipitation in homogeneous and heterogeneous porous media. Water Resources Research. 47, W03513, doi:10.1029/2010WR009677.

Or, D., P. Lehmann, N. Shokri. 2007. Characteristic lengths affecting evaporation from heterogeneous porous media with sharp textural boundaries. Estudios de la Zona No Saturada del Suelo. 8: 1-8.

Or, D. 2008. Scaling of capillary, gravity and viscous forces affecting flow morphology in unsaturated porous media. Advances in Water Res. 31:1129-1136.

Papafotiou, A., R. Helmig, J. Schaap, P. Lehmann, A. Kaestner, H. Flu˙hler, I. Neuweiler, R. Hassanein, B. Ahrenholz, J. To˙lke, A. Peters, and W. Durner.

2008. From the pore scale to the lab scale: 3-D lab experiment and numerical simulation of drainage in heterogeneous porous media. Advances in Water Resources. 31: 1253–1268.

Phillip, J.R. 1957. Evaporation, and moisture and heat fields in soils, Journal of Metrology. 14: 354-366.

Pillai, K.M., M. Prat, and M. Marcoux. 2009. A study on slow evaporation of liquids in a dual-porosity porous medium using square network model. International Journal of Heat and Mass Transfer. 52: 1643–1656.

Roberts, T., N. Lazarovitch, A.W. Warrick, T.L. Thompson. 2009. Modeling salt accumulation with subsurface drip irrigation using HYDRUS-2D. Soil Science Society of America Journal. 73: 233-240.

Rossi, M., O. Ippisch, and H. Flühler. 2008. Solute dilution under imbibition and drainage conditions in a heterogeneous structure: Modeling of a sand tank experiment. Advances in Water Resources 31:1242–1252.

Russo, D., J. Zaidel, and A. Laufer. 1998. Numerical analysis of flow and transport in a three- dimensional partially saturated heterogeneous soil. Water Resources Research. 34: 1451-1468.

Schaap, J. D., P. Lehmann, A. Kaestner, P. Vontobel, R. Hassanein, G. Frei, G.H. de Rooij, E. Lehmann, H. Flühler. 2008. Measuring the effect of structural connectivity on the water dynamics in heterogeneous porous media using speedy neutron tomography. Advances in Water Resources. 31:1233–1241.

Schroth, M. H., J. D. Istok, and J. S. Selker. 1998. Three-phase immiscible fluid movement in the vicinity of textural interfaces. Journal of Contaminant Hydrology. 32: 1–23.

Shahraeeni, E., and D. Or. 2010. Thermo-evaporative fluxes from heterogeneous porous surfaces resolved by infrared thermography. Water Resour. Res. 46: W09511, doi:10.1029/2009WR008455.

Shahraeeni, E., and D. Or. 2011. Quantification of subsurface thermal regimes beneath evaporating porous surfaces. International Journal of Heat and Mass Transfer 54: 4193–4202.

Shaw, T.M. 1987. Drying as an immiscible displacement process with fluid counterflow. Physical Review Letters. 59: 1671-1674.

Shokri, N., P. Lehmann, and D. Or. 2010. Liquid-phase continuity and solute concentration dynamics during evaporation from porous media: Pore-scale processes near vaporization surface. Physical Review E. 81: 046308.

Shokri, N., P. Lehmann, and D. Or. 2009. Characteristics of evaporation from partially wettable porous media. Water Resources Research. 45: W02415, doi:10.1029/2008WR007185.

Shokri, N., P. Lehmann, P. Vontobel, and D. Or. 2008. Drying front and water content dynamics during evaporation from sand delineated by neutron radiography. Water Resour. Res., 44, W06418, doi:10.1029/2007WR006385.

Starr, J. L., A. M. Sadeghi, and Y. A. Pachepsky. 2005. Monitoring and modeling lateral transport through a large in situ chamber. Soil Science Society of America Journal. 69: 1871-1880.

Ursino, N. and T. Gimmi. 2004. Combined effect of heterogeneity, anisotropy and saturation on steady state flow and transport: Structure recognition and numerical simulation. WATER RESOURCES RESEARCH, VOL. 40, W01514, doi:10.1029/2003WR002180.

Ursino, N., T. Gimmi, and H. Fliihler. 2001. Combined effects of heterogeneity, anisotropy, and saturation on steady state flow and

transport: A laboratory sand tank experiment. Water Resources Research. 37: 201-208.

van Genuchten, M. Th. 1980. A closed-form equation for predicting the hydraulic conductivity of unsaturated soils. Soil Science Society of America Journall. 44:892-898.

Vorhauer, N., T. Metzger, and E. Tsotsas. 2010. Empirical macroscopic model for drying of porous media based on pore networks and scaling theory. Drying Technology. 28: 991–1000.

Wildenschild, D., and K. H. Jensen. 1999. Numerical modeling of observed effective flow behavior in unsaturated heterogeneous sands. Water Resources Research. 35: 29-42.

Yiotis, A.G., A.G. Boudouvis, A.K. Stubos, I.N. Tsimpanogiannis, and Y. C. Yortsos. 2003. Effect of liquid films on the isothermal drying of porous media. Physical Review E. 60: 037303.

Yiotis, A.G., A.G. Boudouvis, A.K. Stubos, I.N. Tsimpanogiannis, and Y. C. Yortsos. 2004. Effect of liquid films on the drying of porous media. American Institute of Chemical Engineers Journal. 50:2721-2737.

Yiotis, A. G., I. N. Tsimpanogiannis, A. K. Stubos, and Y. C. Yortsos. 2007. Coupling between external and internal mass transfer during drying of a porous medium. Water Resources Research. 43, W06403, doi:10.1029/2006WR005558

Yiotis, A. G., I. N. Tsimpanogiannis, A. K. Stubos, and Y. C. Yortsos. 2006. Pore-network study of the characteristic periods in the drying of porous media. J. Colloid Interface Sci., 297, 738–748, doi:10.1016/ j.jcis.2005.11.043.

Yoon, H., C. Zhang, C. J. Werth, A. J. Valocchi, and Andrew G. Webb. 2008. Numerical simulation of water flow in three dimensional heterogeneous porous media observed in a magnetic resonance

imaging experiment. Water Resources Research. 44, W06405, doi:10.1029/2007WR006213.

Appendices

Appendix 1

Table of bi-Textures with subsequent t_{Step} times (days). Data obtained from HYDRUS simulation of a soil-water column 50 cm tall x 10 cm wide at a potential evaporation rate of 0.5 cm/day over 100 days. Definition of terms: Sand (S), Loamy Sand (LS), Sandy Loam (SL), Loam (L), Silt (Si), Silt Loam (SiL), Sandy Clay Loam (SCL), Clay Loam (CL), Silty Clay Loam (SiCL), Sandy Clay (SC), and Silty Clay (SiC). Example of abreviation used for texture combination: Loamy Sand & Silt Loam (LS_SiL)

Texture	t_{Step1}	t_{Step2}	t_{Step3}	t_{Step4}	t_{Step5}	t_{Step6}
S_LS	8	13				
S_SL	6.3	6.5	7.7	12.6	16	
S_L	5	5.2	6.5	14.3		
S_Si	4.4	5	8.1			
S_SiL	4.5	4.8	5.6	---	13.6	
S_SCL	5	5.6	6.7	8.2	12.8	
S_CL	4.25	6	16.8			
S_SiCL	4	4.7	10.7			
S_SC	4	5.6				
S_SiC	2.9	4.9				
S_C	3.3	9.1				
Texture	t_{Step1}	t_{Step2}	t_{Step3}	t_{Step4}	t_{Step5}	t_{Step6}
LS_SL	7.2	7.6	8.4	10.8	12.8	
LS_L	5.8	6	7.5	13.3	19	
LS_Si	4.8	5.7	11			
LS_SiL	5	5.3	6.6	13.4	25	
LS_SCL	4.5	9.5				
LS_CL	4.6	5.1	8	14		
LS_SiCL	4.5	11.5				
LS_SC	3.3					
LS_SiC	2	5				
LS_C	3	7				

Texture	t_{Step1}	t_{Step2}	t_{Step3}	t_{Step4}	t_{Step5}	t_{Step6}
SL_L	7.6	13	15.5			
SL_Si	6	10.3	15.6			
SL_SiL	6.9	7.9	11.8	17.3		
SL_SCL	7	8				
SL_CL	5.8	11.2				
SL_SiCL	5.1	9				
SL_SC	4.4					
SL_SiC	5.3	8.3				
SL_C	4.6	7.2	8.5			
Texture	t_{Step1}	t_{Step2}	t_{Step3}	t_{Step4}	t_{Step5}	t_{Step6}
L_Si	8	11.5				
L_SiL	8.9	13				
L_SCL	6.4	7.8	8.8			
L_CL	6.8	7.5				
L_SiCL	5.7	6.5				
L_SC	3	7				
L_SiC	1.4	5.5				
L_SiC	1.4	5.5				
L_C	4.8	5.3				
Texture	t_{Step1}	t_{Step2}	t_{Step3}	t_{Step4}	t_{Step5}	t_{Step6}
Si_SiL	8.9	9				
Si_SCL	4.5	6.9				
Si_CL	5.3	6.4				
Si_SiCL	4.5	5.5				
Si_SC	1.8	4.5	6.1	7.9		
Si_SiC	0.7	5.1				
Si_C	3.7	4.5				

Texture	t_{Step1}	t_{Step2}	t_{Step3}	t_{Step4}	t_{Step5}	t_{Step6}
SiL_SCL	5.3	8.6	10.5	13.2		
SiL_CL	6.4	7.5				
SiL_SiCL	4.5	6.5				
SiL_SC	3.3	6				
SiL_SiC	0.5	5.5				
SiL_C	4.2	4.25				
Texture	t_{Step1}	t_{Step2}	t_{Step3}	t_{Step4}	t_{Step5}	t_{Step6}
SCL_CL	3.4	6				
SCL_SiCL	2.5	4.4				
SCL_SC	3	4.3				
SCL_SiC	1					
SCL_C	2					
Texture	t_{Step1}	t_{Step2}	t_{Step3}	t_{Step4}	t_{Step5}	t_{Step6}
CL_SiCL	2.4					
CL_SC	1					
CL_SiC	~0					
CL_C	2.2					
Texture	t_{Step1}	t_{Step2}	t_{Step3}	t_{Step4}	t_{Step5}	t_{Step6}
SiCL_SC	1					
SiCL_SiC	1	1.5				
SiCL_C	1					
Texture	t_{Step1}	t_{Step2}	t_{Step3}	t_{Step4}	t_{Step5}	t_{Step6}
SC_SiC	0.3					
SiC_C	~0					

Appendix 2
Results from Hydrus simulation of evaporation rate and cumulative

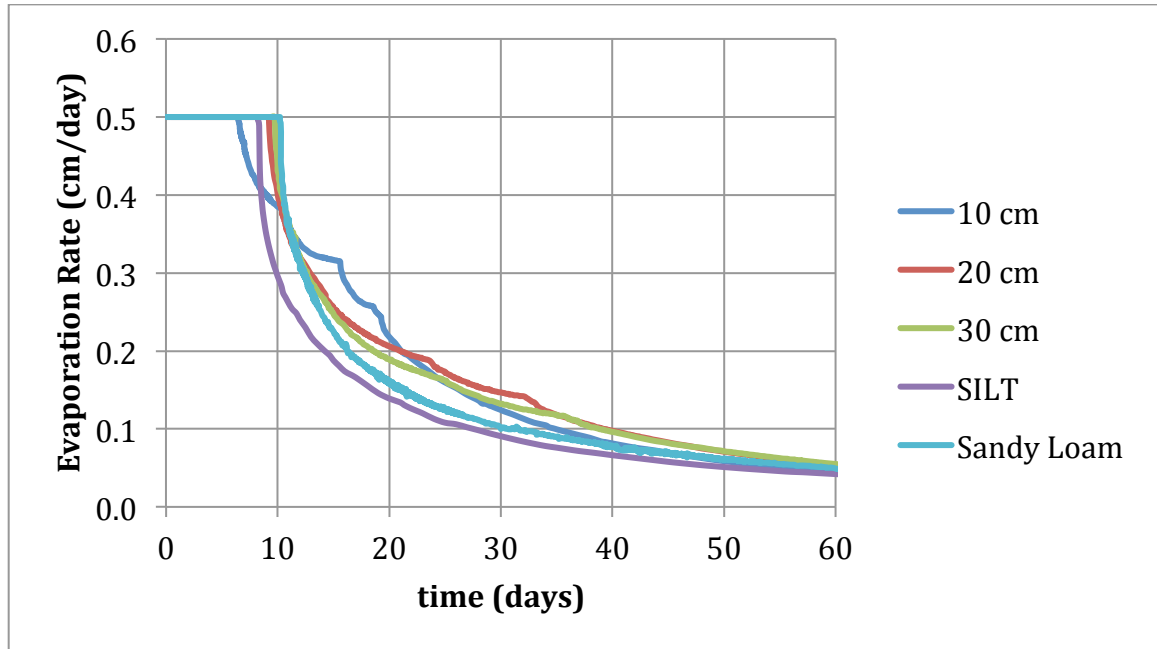evaporative losses from bi-texture of varying coarse width.

Figure 23: Evaporation rate of Sandy Loam & Silt for varying degrees of
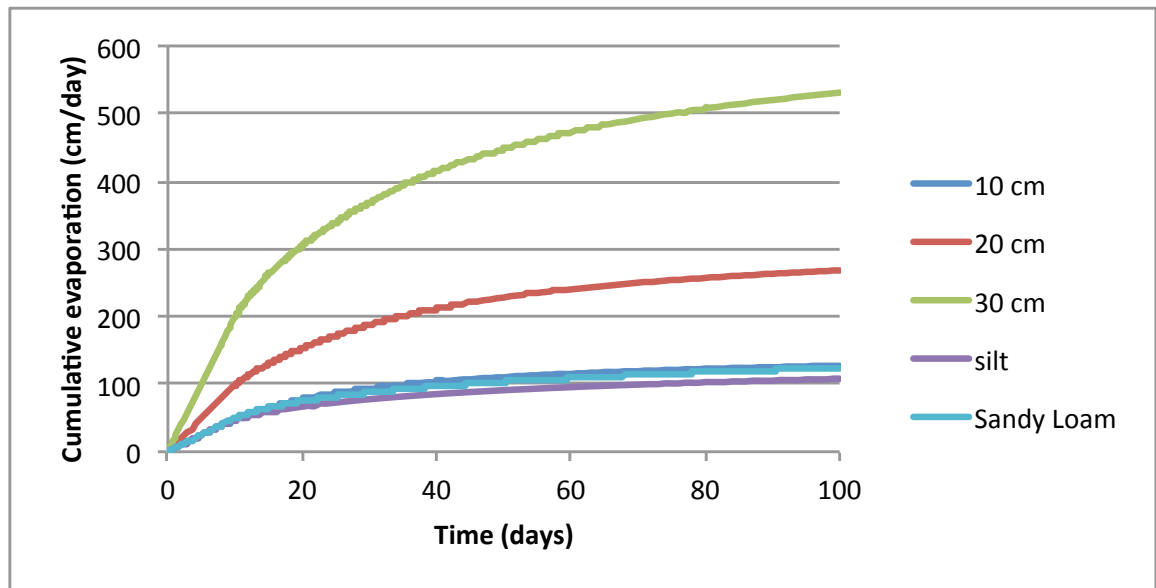depth of coarse portion (10 cm, 20 cm, and 30 cm).

Figure 24: Results from Hydrus simulation showing cumulative evaporation loss over time of Sandy Loam & Silt for varying widths of coarse portion.